TESI DOCTORAL

BRAIN VOLUME AND BRAIN METABOLITE CHANGES IN THE FIRST STAGES OF PRIMARY PROGRESSIVE MULTIPLE SCLEROSIS

A short-term longitudinal study

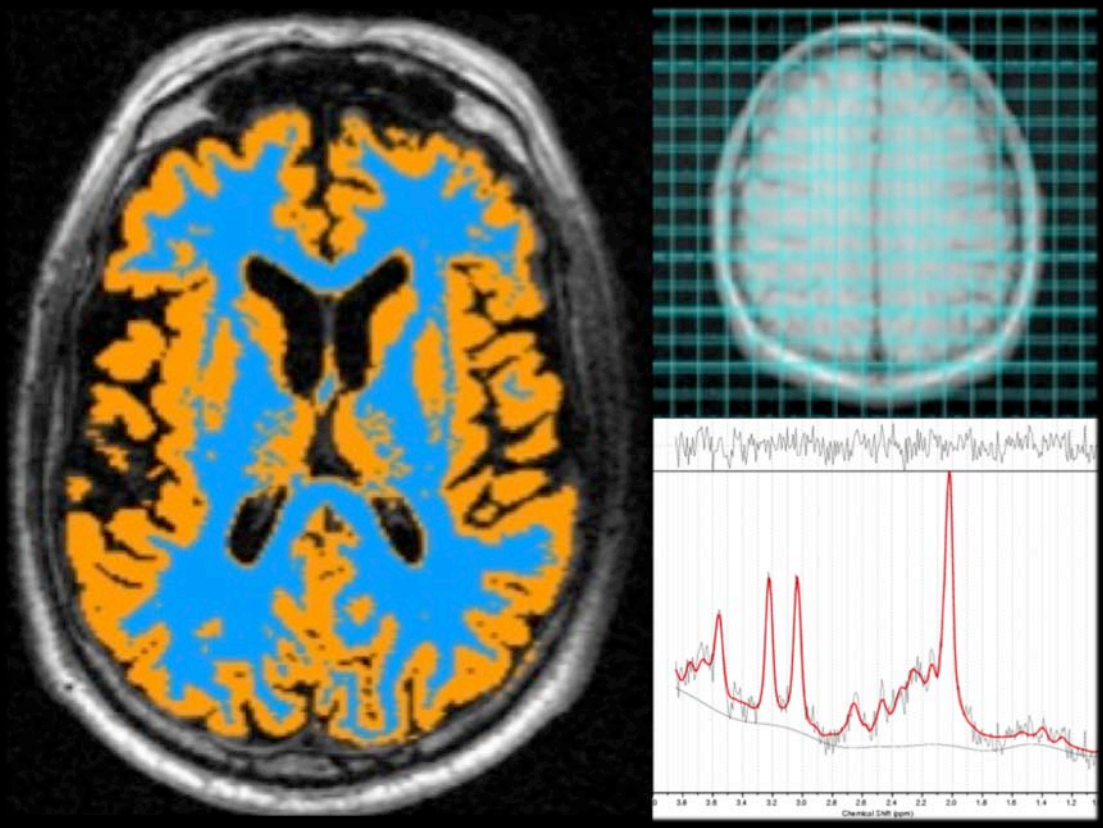

Doctorand

Jaume Sastre Garriga

Director

Prof. Xavier Montalban Gairín

UAB Universitat Autònoma de Barcelona

Cemcat

TESI DOCTORAL

BRAIN VOLUME AND BRAIN METABOLITE CHANGES IN THE FIRST STAGES OF PRIMARY PROGRESSIVE MULTIPLE SCLEROSIS

A short-term longitudinal study

Doctorand

Jaume Sastre Garriga

Director

Prof. Xavier Montalban Gairín

Tutor

Prof. Vicent Fonollosa i Pla

Programa de Doctorat en Medicina Interna

Departament de Medicina - Facultat de Medicina

Universitat Autònoma de Barcelona

Barcelona, 2015

Les carreres per les quals l'amic encerca son amat
són llongues, perilloses,
poblades de consideracions,
de sospirs e de plors,
e enluminades d'amors

Llibre d'Amic e Amat
Ramon Llull

1. FOREWORD

1.1 Acknowledgements

Completion of this doctoral thesis was possible with the support of a long list of people. I would like to express my most sincere gratitude to all of them. I am sure I will be missing some names and I do apologize. Maybe you are not in my hippocampus right now, but you are for sure in my heart.

Al meu amic, el Professor Xavier Montalban, director d'aquesta tesi, cap de Servei de Neurologia / Neuroimmunologia i del Cemcat, que ha permès fer realitat tot això. Estímul immens tant personal com científic, sempre cercant una mica més enllà del que és possible, fins que és possible. Qualsevol agraïment quedarà curt. Amb estimació... i *enjundia*.

To Professor AJ Thompson, he has been key in many ways for me to reach the goal of completing this doctoral thesis for which he has been a true director. For his friendship and scientific support and guidance during my stay in London as a member of his team. Without his sheer tenacity I would have quit in too many occasions. Cheers, Alan!

To my friends and colleagues at the Institute of Neurology, in London, for their personal support and technical guidance throughout. Big thanks to Olga Ciccarelli, who was always there to help me when I, too often, was getting stuck with my analysis. Many thanks as well to Declan Chard, Ahmed Toosy, Mara Cercignani, Lluís Ramió-Torrentà and Gordon Ingle. I also want say thanks to Dr. Mary McLean, for her help in the spectroscopy data analysis and acquisition, and to Mr. Christopher Benton and Ms. Ros Gordon who acquired all the images needed for this thesis.

Als meus companys i amics del Cemcat i de la Unitat de Ressonància Magnètica a l'Hospital de la Vall d'Hebron, que m'han ensenyat tantes i tantes de coses sobre

l'esclerosi múltiple, la ressonància magnètica i la vida, així en general. Estic orgullós i content d'haver gaudit de l'amistat de Na Mar Tintoré, N'Àlex Rovira, En Carlos Nos, N'Ingrid Galán, Na María Jesús Arévalo, En Jordi Río, Na Déborah Pareto, En Manuel Comabella, Na Carmen Espejo, Na Carme Tur, N'Àngela Vidal-Jordana, Na María José Vicente, Na Rosalía Horno, Na Mila Fraga, Na Dúnia Muñoz i En Josep(h) Graells. Esper seguir-ho fent durant els anys a venir, que encara tenc moltes de ganes de seguir aprenent. Un agraïment molt especial a Na Imma Pericot, companya dels anys de formació com a neuròleg, amb qui sempre he tengut la sort de poder comptar, per a tot. A tots els amics i companys del Cemcat, d'abans i d'ara, gràcies!

Tenc un grapat d'amics que estim molt i que, com solen fer *ets* amics, m'han acompanyat en més d'una aventura que m'ha fet esser així com som. Qualcuna part d'aquesta tesi segur que és *culpa* den Llorenç, en Christian, en Jordi, en Javi, en Miquel Àngel, en Xisco, en Pep, en Pina,...

A Menorca i a Mallorca.

A Na Sònia, que me va acompanyar en els anys a Londres, on vaig poder fer tot el treball relacionat amb aquesta tesi, i que m'ha acompanyat en els anys, una mica massa llargs, que m'ha costat escriure-la i que sempre ha estat un estaló imprescindible en tot allò que he volgut o hagut de fer. Hem tengut dos fills preciosos, En Bià i En Toni, que de moment s'estimen més llegir En *Geronimo Stilton* que aquesta tesi, però tot arribarà.

A ma mare i mon pare, En Rafel i Na Mary, els hi he d'agrair tot, així que me pareix una miqueta ridícul fer-ho de manera específica per aquesta tesi doctoral. Però ho faig de tot cor, perquè *sa* darrera passa és important, però més ho són totes aquelles que te deixen en posició de fer-la. Una besada ben forta per ells i també *pes* meu germà, En Sebastià.

1.2 Glossary

3DFSPGR 3D inversion-prepared fast spoiled gradient recall

BICCR Brain-to-intracranial capacity ratio

BPF Brain Parenchymal Fraction

CSI Chemical Shift Imaging

Cho Choline

CRMVB Cramer Rao Minimum Variance Bounds

Cr Creatine

CSF Cerebrospinal Fluid

DIS Dissemination in Space

DIT Dissemination in Time

DSS Disability Status Scale

DTI Diffusion Tensor Imaging

EDSS Expanded Disability Status Scale

FOV Field of View

fMRI functional Magnetic Resonance Imaging

GA Glatiramer Acetate

Gd Gadolinium

Glx Glutamate-Glutamine

GM Grey Matter

GMF Grey Matter Fraction

HLA Human Leukocyte Antigen

IgG Immunoglobulin G

Ins Inositol

LCModel Linear Combination Model

MAGNIMS Magnetic Resonance in Multiple Sclerosis

MS Multiple Sclerosis

MR Magnetic Resonance

MRI Magnetic Resonance Imaging

MRS Magnetic Resonance Spectroscopy

MRSI Magnetic Resonance Spectroscopy Imaging

MTI Magnetization Transfer Imaging

MSFC Multiple Sclerosis Functional Composite

NAA N-acetyl-aspartate

NAWM Normal Appearing White Matter

NEX Number of Excitations

NHPT Nine-Hole Peg Test

PASAT Paced Auditory Serial Addition Test

PBVC Parenchymal Brain Volume Change

PD Proton Density

PPMS Primary Progressive Multiple Sclerosis

PRESS Point Resolved Spectroscopy

PRMS Progressive Relapsing Multiple Sclerosis

RCT Randomized Clinical Trial

RRMS Relapsing-Remitting Multiple Sclerosis

SIENA Structural Image Evaluation using Normalization of Atrophy, longitudinal

SIENAx Structural Image Evaluation using Normalization of Atrophy, cross-sectional

SPM Statistical Parametric Mapping

SPMS Secondary Progressive Multiple Sclerosis

ST Slice Thickness

STEAM Stimulated Echo Acquisition Mode

TE echo time

tNAA total N-acetyl-aspartate

TPMS Transitional Progressive Multiple Sclerosis

TR repetition time

TWT Timed Walk Test

VEP Visual Evoked Potentials

WM White Matter

WMF White Matter Fraction

2. BACKGROUND

2.1 Multiple Sclerosis and its clinical forms

Multiple Sclerosis (MS) is the prototypical chronic inflammatory demyelinating disease of the central nervous system[1, 2]. It is important to highlight that through acute inflammation-related damage or due to long-standing sub-lethal damage a relentless neurodegenerative process also takes place[3]. It is widely accepted that the acute and overt inflammatory process present in MS is responsible for the transient neurological deficits observed in MS relapses, whereas the progressive accumulation of disability is related to the neurodegenerative process.

Multiple sclerosis was first described in the XIX century through the work of JM Charcot and others like Vulpian and von Frerichs[4], although a fairly detailed earlier account exist in the writings of Sir Augustus d'Esté, grandson of King George III of England and affected by MS, who left in his personal diary a detailed description of the relapsing symptoms and accumulating disability he endured through the years. One of the first descriptions of the disease was done by Robert Carswell in 1838 when he reported the existence of "*a remarkable lesion of the spinal cord accompanied with atrophy*"[2, 5], but it was JM Charcot who first defined the existence of two main clinical forms of MS: relapsing-onset and progression-onset. Although general agreement on such classification existed for many years "*there was no unanimous agreement on definitions for the various clinical subtypes of MS*" as stated by Lublin and Reingold in their landmark Neurology paper[6]. In this paper, based on the results of a survey among MS experts worldwide, a consensus was reached to define four main clinical forms of MS. Relapsing-onset forms of MS included relapsing-remitting MS (RRMS) and secondary progressive MS (SPMS). Patients with RRMS experience episodes of neurologic deficit (attacks, relapses, bouts) that may or may not fully recover (remission). Patients with SPMS experience a relentless accumulation of neurological disability after a period of relapses and remissions. Of note that all patients labelled as having SPMS have previously gone through a RRMS phase, but in contrast a number of patients with RRMS will never

enter a secondary progressive phase of the condition. Progressive forms of MS included primary progressive MS (PPMS) and progressive-relapsing MS (PRMS). Patients with PRMS were defined as those with "*progressive disease from onset, with clear acute relapses, with or without full recovery; periods between relapses characterized by continuing progression*". PPMS will be defined in the next section. Recent challenges to this 20 year-old classification arise from all knowledge acquired with the use of Magnetic Resonance Imaging (MRI) as well as by the definition of new MS phenotypes, not yet fully appraised in the early nineties. A task force has recently produced a new classification of MS that has superseded the one abovementioned[6]. Briefly, the PRMS form disappears and activity measured by relapses or MRI activity and disability progression are key points[7].

Most research in the field of MS has been performed in RRMS and relapsing phenotypes. A reason for that is the higher prevalence of this clinical form of MS. A further reason is the inherent difficulties in the definition and timeframe of the relevant clinical outcomes in PPMS as compared to RRMS. However, PPMS offers a unique opportunity to investigate the neurodegenerative component of MS and its relation to progression of disability in MS. The works presented in this doctoral thesis are part of a wider project devoted to further explore the clinical and radiological counterparts of the MS neurodegenerative process using PPMS as the best available model.

2.2 Primary Progressive Multiple Sclerosis

2.2.1 Definition and clinical and epidemiological features.

As mentioned previously, PPMS is the clinical phenotype of MS that is characterized by progressively worsening disability in spite of the absence of clinical relapses; the most widely accepted definition of PPMS is the one that features in the consensus

paper by Lublin and Reingold, and is as follows: "*Disease progression from onset with occasional plateaus and temporary minor improvements allowed*"[6]. Most series indicate that PPMS patients may represent between 5% and 20% of the total number of MS patients[8, 9]. Main epidemiological differences between PPMS and RRMS relate to age at onset and gender distribution: whereas mean age at onset for RRMS is 30 years[10], in PPMS is 40 years[8]; on the other hand, there is no gender predominance in PPMS[9] as compared to the female predominance in RRMS[10], which has been shown to be increasing recently[11]. Most PPMS patients present with a clinical picture of progressive paraparesis (and more rarely hemiparesis), and very infrequently patients may have a clinical onset of progressive visual loss, progressive cerebellar or brainstem syndromes or progressive cognitive disturbance[12].

2.2.2 Genetics

A genowide association study of MS that examined a significant fraction of common variations in the human genome definitely confirmed the genetic component of MS susceptibility; this study reported a series of genetic alleles associated with a higher risk of MS: interleukin-2 receptor alpha gene, interleukin-7 receptor alpha gene, and of course the HLA locus[13]. Even though a number of studies have implicated some specific genetic variants in the risk of developing PPMS as compared to RRMS subjects as well as controls[14-17], definite differences associated with these phenotypes at the major histocompatibility complex or elsewhere in the genome have not been found[18]. Provided that genetic variants identified till now have only a minor effect on susceptibility to MS, it is to be expected that differences between RRMS and PPMS will be of the same magnitude and thus a very large sample of patients with PPMS will need to be recruited to have a meaningful option of finding differentially associated alleles[18] if these exist[19]. If encountered, such differences might provide the basis for future targeted therapies in PPMS.

2.2.3 Natural history

Progression rates have been investigated through long-term follow-up studies of large cohorts, mainly those from London (Ontario, Canada), British Columbia (Canada) and Lyon (France). Cottrell et al.[20] reported a natural history study of 216 PPMS patients from London, Ontario, with a mean follow-up of 23.7 years, and a median time to disability status score (DSS) 6 and DSS 8 of 8 and 18 years, respectively; negative prognostic factors included shorter time to DSS 3 and involvement of three or more neurological systems at onset. Two other findings from this study[20] are also worth mentioning: progression rates were found to be faster in SPMS as compared to PPMS and up to 28% of patients with PPMS experienced relapses even decades after onset of progression. Tremlett et al.[9] reported a natural history study of 352 PPMS patients from British Columbia, Canada, with mean disease duration of 17 years. Patients experiencing relapses over the observation period were not considered. Although 25% of patients had reached Expanded DSS (EDSS) 6.0 after a mean time of 7 years after disease onset, 25% were still EDSS 5.5 or less after 25 years. Interestingly, these progression rates are considerably lower than those reported by Cottrell et al.[20]. Conversely, negative predictive factors were similar to those reported by Cottrell et al.[20]: "sooner to cane, sooner to wheelchair" (a shorter time to EDSS 6 predicted a shorter time to EDSS 8). Finally, Confavreux et al.[21] reported a natural history study including 173 PPMS patients from Lyon, France with mean disease duration of 9.6 years. In this study, patients with superimposed relapses were categorized as progressive relapsing; in all, 39% of patients with a progressive course from onset went on to develop relapses over the period of observation; according to the new classification these patients would now be categorized as PPMS with activity[7]. In contrast to the results reported by Cottrell et al., in the Lyon cohort no differences are observed in disease progression rates between relapsing and progressive onset MS (including PPMS and relapsing-progressive MS) who have entered a progressive course. A further finding of the Lyon study would indicate that progression might be an age-dependent phenomenon, as age at onset of progression seems to be similar in both groups of

patients. This has been later on confirmed in further analyses of the London, Ontario database[22, 23].

2.2.4 Pathological findings and pathogenesis

There is a dearth of specific data on the pathology of PPMS. Reported data might point to the presence of a specific immunopathological subtype of primary oligodendrocyte degeneration in a subgroup of PPMS patients; this immunopathological subtype would not be present in relapsing patients[24]. Overall, pathological specimens of patients with PPMS would tend to display less severe inflammation, more prolonged T-cell infiltration, more pronounced oligodendrocyte loss, and a maintained low-level of axonal damage as compared to patients with relapsing onset MS[24].

More recently, Magliozzi et al.[25] described the absence of meningeal B-cell follicles in PPMS as compared to a prevalence of 41% in patients with SPMS; this latter group of follicle-positive patients were found to be more aggressive and displaying more severe cortical demyelination. In any case, cortical demyelination seems to be profound in patients with PPMS and also related to meningeal inflammation, as reported by Kutzelnigg et al.[26]. In the same study, the authors described a mild but diffuse inflammatory reaction in the normal appearing white matter (NAWM) of patients with SPMS and PPMS, which was less marked in acute and relapsing MS, and seemed to be related to an intense microglial activation and significantly more diffuse axonal damage in the NAWM as compared to patients with acute and relapsing disease[26]. Conversely, active plaques were found to be predominantly formed in patients with acute or relapsing MS, and tended to be either inactive or showed slow expansion on their edges in progressive multiple sclerosis. In contrast to what had been described previously, these authors did not find instances of primary demyelination in PPMS[26]. In this study, the only significant differences between SPMS and PPMS were a lower lesion load and lower number of

inflammatory infiltrates in white matter in PPMS patients[26]. Such a complicated picture may be responsible for the lack of a definitive pattern of immunological features in PPMS as compared to relapsing MS; whereas some studies have found differences in the components of the pathogenetical process, some others have not[27]. In all, the unifying concept of MS seems to be also plausible according to pathological and immunological data[27].

2.2.5 Differential and positive diagnosis

Differential diagnosis of PPMS needs to take into account conditions that may present with a progressive spastic paraparesis[12, 19]; as mentioned before, progressive visual, cerebellar, brainstem or cognitive syndromes are extremely rare and a diagnosis of PPMS in those settings is utterly challenging. A recent consensus paper on the differential diagnosis of MS was mostly based on relapsing onset MS and, thus, is not helpful when a suspicion of PPMS is raised[28]. There are a number of radiological features (*red flags*) that, if appear in patients presenting with a clinical picture compatible with PPMS, may be helpful to reduce the chances of a false positive diagnosis. The concept of no better explanation is expanded in a recent paper reviewing a number of radiological characteristics considered to be not suggestive of MS[29].

Once any conditions that may mimic MS have been reasonably ruled out, a positive diagnosis of PPMS can be done using available diagnostic criteria. The early 80's Poser's criteria[30] were not dealing with appropriate specificity with PPMS nor they were incorporating in an operational way all recent advances from MRI research and were subsided by those published in 2000 by Thompson and colleagues[31]. Very briefly, in that set of criteria, in patients presenting with a progressive syndrome for one year or more, in which other conditions had been excluded and in the absence of relapses or remissions, the presence of oligoclonal bands in cerebrospinal fluid (CSF) was mandatory for a diagnosis of *definite* PPMS, which could be achieved

when the MRI was positive (nine or more brain lesions and/or two or more spinal cord lesions and/or four to eight brain lesions in combination with one spinal cord lesion) or when the MRI was equivocal (four to eight brain lesions or one to three brain lesions in combination with one spinal cord lesion) coupled with a delayed visual evoked potential (VEP). The criteria by Thompson and colleagues[31] were included with almost no changes in the 2001 version of the McDonald criteria[32], except by the possibility of demonstrating dissemination in time (DIT) with MRI instead of one year of prospectively assessed clinical progression.

The 2005 version of the McDonald criteria[33] did introduce significant changes in relation to the 2001 version, namely the possibility of reaching a diagnosis in the absence of oligoclonal bands in CSF. A diagnosis of PPMS according to McDonald 2005 diagnostic criteria required the presence of two out of the three following criteria: 1. Positive brain MRI (nine T2 lesions or four or more T2 lesions with a delayed VEP); 2. Positive spinal cord MRI (two focal T2 lesions); 3. Presence of oligoclonal bands in CSF. In this set of criteria disease progression could be determined either prospectively or retrospectively.

The McDonald 2010 diagnostic criteria[34] followed on previous demonstration that the performance of dissemination in space (DIS) criteria used in RRMS was very similar to the 2005 PPMS criteria[35], and thus allowing for a unification of requirements for DIS between RRMS and PPMS. A diagnosis of PPMS according to McDonald 2010 criteria require the presence of one year of disease progression (retrospectively or prospectively determined) plus 2 out of three of the following requirements: 1. Evidence for DIS in the brain based on at least one T2 lesion in at least one of these three areas (periventricular, juxtacortical, infratentorial); 2. Evidence for DIS in the spinal cord based on two or more T2 lesions; 3. Positive CSF (presence of oligoclonal bands or raised Immunoglobulin G –IgG- index). Overall, in the last decade great advance has been made in operationalizing the diagnosis of PPMS. In spite of that, there is still a long way to go, namely with regards to enhancing the evidence base

which supports the present algorithm and to further the schemes for the differential diagnosis of PPMS, which still remain a great challenge for the clinical neurologist.

2.2.6 Treatment aspects

There is no treatment approved for PPMS. Such a discouraging sentence is based on the constantly failed randomized clinical trials performed in PPMS which, it is fair to say, are by far outnumbered by those performed in RRMS.

Interferon-beta 1a and 1b have been tried in double-blind randomized clinical trials (RCT), although both trials have been clearly underpowered to detect treatment effects. Leary et al[36] performed a RCT on 50 patients with PPMS that were randomized to receive weekly intramuscular interferon-beta 1a (in two doses of 30 or 60 micrograms) or placebo for two years. The primary endpoint was the time to sustained disability progression. Secondary outcomes included Multiple Sclerosis Functional Composite (MSFC) subtests, and on MRI, T2 and T1 brain lesion volumes and brain and spinal cord atrophy. Issues of low tolerability of the 60-microgram dose were raised as flu-like reactions were considered to be severe and elevations of liver enzymes were observed, but no other safety concerns were identified. No treatment effect was observed on the primary endpoint. However, some hints of efficacy were found for secondary outcomes as patients on low dose of interferon-beta 1a had a lower rate of accumulation of T2 lesion volume than controls ($p=0.025$). A possible pseudoatrophy effect was seen, as patients on the higher dose of interferon had greater atrophy rates (ventricular volume, $p=0.025$). Montalban et al[37], performed a double-blind RCT in 49 patients with PPMS and 24 patients with so-called 'transitional' progressive (TP) forms of MS; TP forms of MS were defined as those patients with a progressive course and a single relapse before or during progression[38]. The 73 patients studied were randomized to receive either interferon-beta 1b (dose of 8 MIU) or placebo for 24 months. For this study, the main objective was safety and tolerability of interferon-beta 1b. The primary efficacy variable was

the time to neurological deterioration (using the EDSS), with confirmation at 3 months. Whereas more patients in the treatment arm had at least one related adverse event (94.4% versus 45.9%; p< 0.001) no other significant differences in safety endpoints were observed. Time to neurological deterioration as measured by the EDSS was not different between trial arms (p=0.31). However, similar to results reported by Leary et al[36], statistically significant differences favouring the treatment arm were observed for a number of secondary outcomes, including the MSFC score at several timepoints, T1 and T2 lesion volume changes at 12 and 24 months, mean number of active lesions and proportion of patients with active lesions at 24 months. In all, this was considered to be a negative study, as no beneficial effect on EDSS progression was demonstrated, but a hint of efficacy of interferon-beta 1b was undeniable given the positive results obtained in a number of MRI secondary outcomes. Findings after five years of trial termination support this notion as modest but beneficial effects of interferon-beta 1b on clinical variables and brain atrophy development were observed[39].

Wolinsky and coworkers[40], performed a multi-centre double-blind RCT in patients with PPMS that were randomized to receive glatiramer acetate (GA) or placebo. This trial was not underpowered as sample size was 943 and had a longer duration (3 years) than the previous two, but the final results were also negative, as no significant differences were observed in the primary outcome measure, the time to sustained accumulated disability (using EDSS confirmed at three months), between GA and placebo arms (p=0.17). However, again small hints of efficacy were obtained in the analysis of the secondary MRI outcomes, as significant decreases in enhancing lesions in year 1 and smaller increases in T2 lesion volumes in years 2 and 3 were observed in the GA arm versus placebo. On the contrary, there were no differences between treatment groups in changes from baseline in T1 lesion volume or in brain volume.

Riluzole, an inhibitor of glutamate transmission that has been extensively used in amyotrophic lateral sclerosis, has been also tested in PPMS in a very small non-

controlled pilot study including 16 PPMS patients[41]. Riluzole was seen to be safe and cervical cord area loss, which proceeded at a speed of 2% during the first year seemed to stabilize during the second year (-0.2%). No controlled studies have been performed so far using this agent in PPMS and its possible neuroprotective effect remains largely untested.

Rituximab, a monoclonal antibody against the surface molecule CD20, causing a rapid and intense depletion of B-cells, has also been tried in a two-year double-blind RCT involving 439 patients with PPMS[42]. The primary endpoint, time to confirmed EDSS progression confirmed at three months, was negative (p=0.14), although subgroup analyses showed a significant effect in patients aged less that 51 years and also in those with gadolinium(Gd)-enhancing lesions at baseline. Positive results in MRI secondary outcomes were also observed and no unexpected adverse effects of the drug were recorded. As a follow-up of this trial a large phase III double-blind international (approximately 210 countries) multicentre RCT of a humanized anti-CD20, ocrelizumab, is now ongoing, aiming to include 630 patients of disease duration less than 15 years (less than 10 years if EDSS lower than 5.0). In this study patients have been randomized to receive (2:1) ocrelizumab 600 mg intravenous every 24 weeks, administered as dual infusions of 300 mg separated by 14 days or placebo infusions. The primary efficacy outcome for this study is the time to onset of sustained disability progression confirmed at 12 weeks. Disability progression is defined by an increase of 1.0 or more EDSS points from baseline if baseline EDSS was of 5.5 or less, or by an increase of 0.5 or more EDSS points from baseline if baseline EDSS was above 5.5.

Another drug in present testing in PPMS is fingolimod, a sphingosine 1-phosphate receptor modulator that blocks lymphocyte egression from lymph nodes thus impairing immune responses. Fingolimod has been successfully tried in RRMS where it was the first oral drug to be marketed worldwide[43-45]. Fingolimod is being tried in a large double-blind placebo-controlled RCT in PPMS patients with less than 10 years of disease duration and baseline EDSS between 3.5 and 6.0. The estimated

enrolment figure is 950 patients and the primary outcome measure is the time to sustained disability progression for patients treated for at least 36 months.

Recently, results from a phase 2A study using natalizumab in patients with progressive MS have been reported[46]. This was an open-label phase 2A study in which 24 patients (12 SPMS and 12 PPMS) were treated with natalizumab for 60 weeks. Seventeen patients completed the study and no new safety issues were reported. Significant decreases in ostepontin levels were found and MRI evidence of improvement was observed. A phase III clinical trial with natalizumab in SPMS is now ongoing, but no clinical trial seems to be ongoing in PPMS with natalizumab.

At present date, in the database clinicaltrials.gov four other drugs feature as in testing in patients with PPMS (an immunomodulating microparticle called MIS416, idebenone, ibudilast and masitinib), but no results have been published yet for any of the trials. A trial with laquinimod in patients with PPMS is also at the planning stage, but has not been introduced yet in the abovementioned database; laquinimod has obtained beneficial effects on disability progression in two large phase III trials in patients with RRMS[47, 48]. Finally, a previous trial of mitoxantrone in PPMS which was known to be largely negative has not yet been published[19].

Finally, in spite of the lack of evidence in favour of treating patients with PPMS with any disease-modifying drug, a recent case-based survey[49] administered to 75 MS specialists in the United States of America revealed that 85% of practitioners would start therapy on a patient with PPMS presenting with Gd-enhancing lesions on their brain MRI with or without spinal cord lesions. Reflecting the lack of evidence and highlighting the unmet need in this field, no consensus was reached on which therapy to start[49].

2.3 Atrophy and Spectroscopy MR techniques

A number of Magnetic Resonance (MR) techniques have been developed in recent years to measure the neurodegenerative process that is a common feature in a number of pathologies affecting the central nervous system. Atrophy and spectroscopy are two of the most widely used techniques to assess this process. Whereas brain atrophy techniques focus on obtaining accurate measurements of distances, areas or volumes of global or regional structures of the brain, spectroscopy techniques focus on obtaining accurate measurements of the molecular components of brain tissue. The works presented in this doctoral thesis will investigate the neurodegenerative component of MS and its relation to progression of disability by applying atrophy and spectroscopy techniques in a cohort of PPMS.

2.3.1 Atrophy MRI techniques

In some instances atrophy assessments can be reliably performed on 2D acquisitions, but the present recommendation is to use isotropic 3D pulse sequences[50]. Although qualitative assessments can be obtained using visual ratings[51], brain atrophy measures are usually based on either two-dimensional or three-dimensional quantitative assessments.

Most **two-dimensional techniques** involve linear measurements, but may also involve surface measurements on a given number of brain slices (which can also be considered as three-dimensional segmentation-based techniques). A number of approaches have been developed, including: measurement of brain width on axial brain MRI slices[52], third ventricle width[52], lateral ventricle width[52], corpus callosum area[52], measurement of the surface of the seven slices rostral to the velum interpositum[53]. A linear measurement is also obtained using the Freesurfer® software, which renders an estimate of cortical thickness[54].

Three-dimensional techniques are usually divided in segmentation-based and registration-based[55, 56]. Segmentation-based techniques are most usually applied in cross-sectional settings and are usually driven by differences in voxel signal intensity as well as location; using segmentation-based techniques voxels are classified into different subtypes (brain / non-brain, CSF / brain, CSF / white matter (WM) / grey matter (GM)). Registration-based techniques are specially suited to be applied in longitudinal designs as they base their algorithms on the detection of changes between serially acquired MRI scans; for that purpose they are superior to segmentation-based techniques as measurement errors tend to be larger in serial studies using several cross-sectional measurements instead of a single measure of change between MRI scans. However, registration-based techniques do not usually allow for calculation of changes in brain tissue types.

Segmentation-based techniques

The so-called brain parenchymal fraction (BPF) technique was initially described by Rudick and coworkers[57]; in this technique the total brain parenchymal tissue is segmented and its fraction to the total volume contained into the brain surface contour determined to obtain a normalized measure of atrophy. The brain-to-intracranial capacity ratio (BICCR)[58] technique is very similar in its principles to the the BPF technique, allowing calculation of the BPF, as many other segmentation techniques, sometimes inducing confusion between BPF as a technique and BPF as an atrophy measure. The Statistical Parametric Mapping (SPM) software[59] was initially developed at the Department of Cognitive Neurology in London to be applied in the analysis of Positron Emission Tomography images and, unlike the other two techniques previously described, is available for free on the software webpage (http://www.fil.ion.ucl.ac.uk/spm/). The SPM software allows segmentation of brain tissue into different subtypes (CSF, WM and GM) using voxel intensity and location features after correction for image intensity inhomogeneity and normalization to a standard brain template (from the Montreal Neurological Institute). Using SPM, BPF

as well as GM and WM fractions (GMF and WMF) can be obtained with good reproducibility (Figure 1)[60].

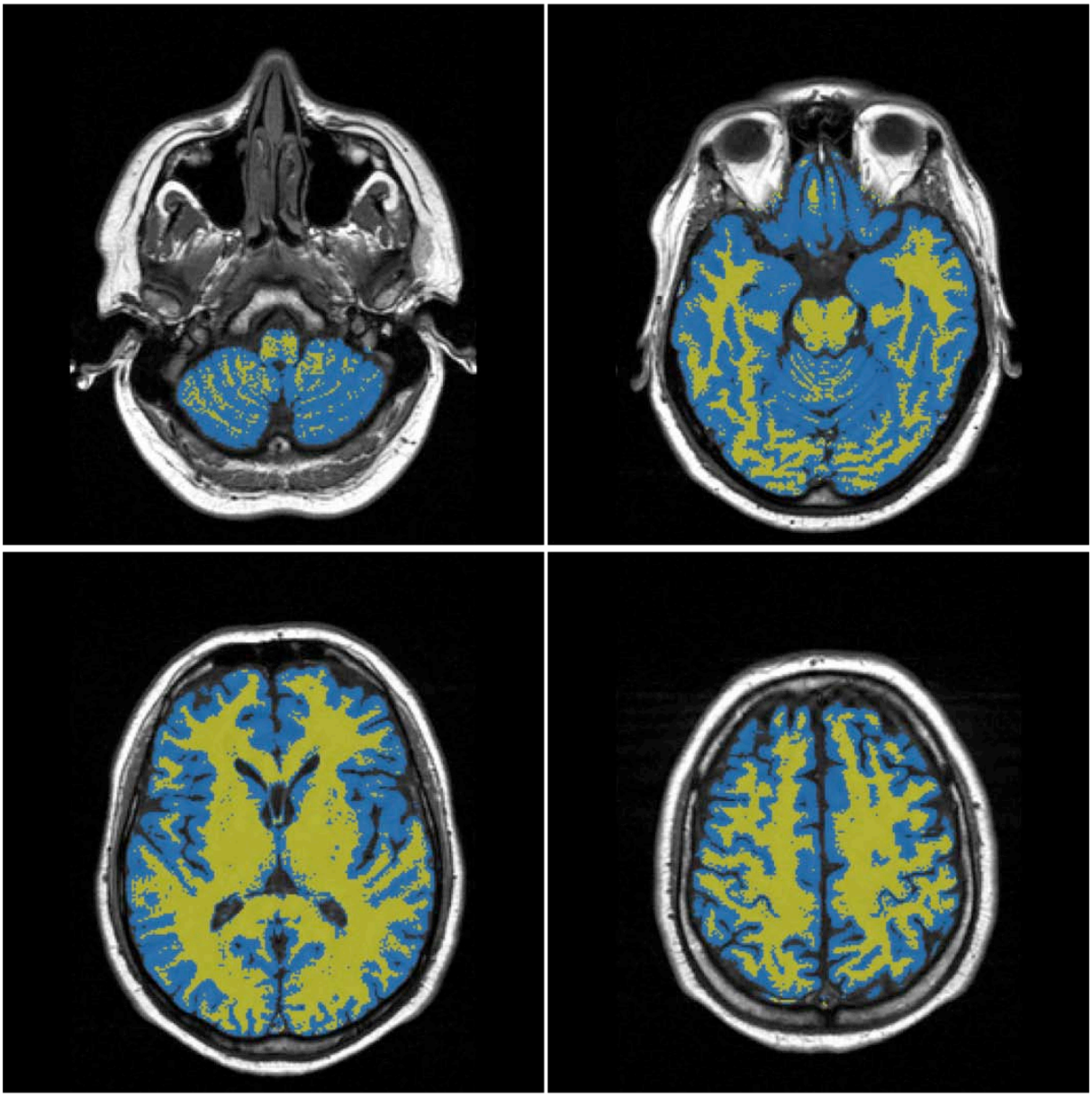

Figure 1. Example of grey (blue) and white (yellow) matter segmentation performed with SPM-based software. Tissue probability masks are created (0 to 100% probability of a voxel pertaining to a given tissue type) and outputs are binarized so that voxels with more than 50% probability of belonging to a given tissue are assigned to that specific tissue type. Voxels for each tissue type are counted and divided by the total number of voxels within the brain cavity to provide a percentage of each tissue to the total intracranial volume. Such approach allows cross-sectional comparisons across different individuals regardless of head size.

The SIENAx software[61] (Structural Image Evaluation, using Normalization, of Atrophy) estimates total brain tissue volume (including separate estimates of volumes of grey matter and white matter), from a single image, normalised for skull size; in this regard it does not provide a measure of the BPF. Other segmentation-based techniques are those based on fuzzy connectedness approaches[62], on histogram segmentation[63] and the MIDAS technique[64]. Agreement between techniques tends to be moderate and, thus, usage of strictly the same technique for all time-points in longitudinal analyses is imperative to avoid spurious findings (Figure 2).

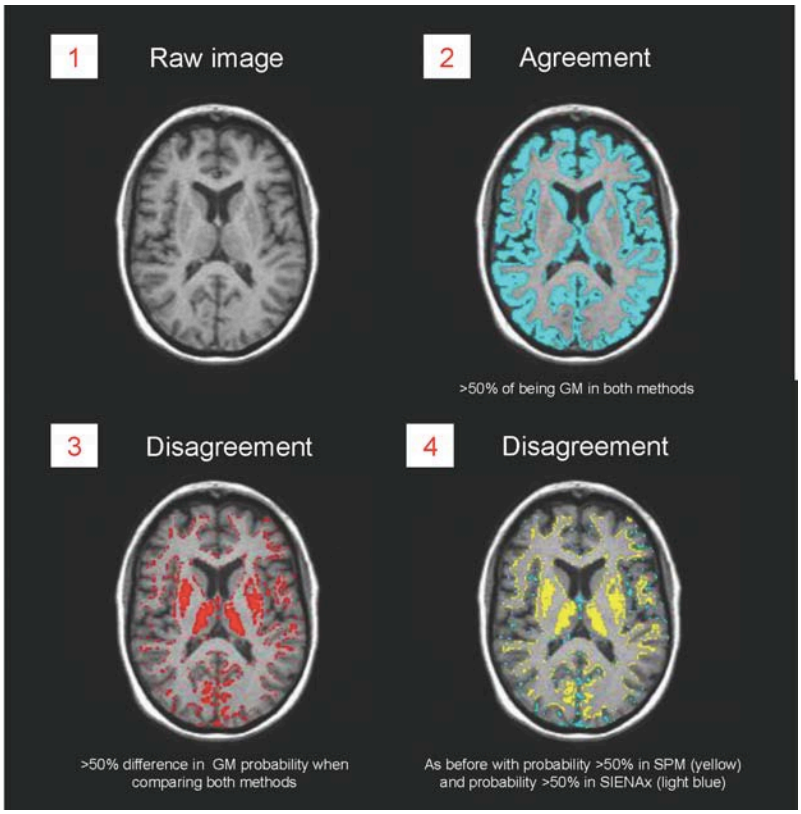

Figure 2. Comparison of grey matter segmentation performed with SIENAx and SPM-based techniques. The raw image (1) is segmented and voxels of more than 50% assigned probability of belonging to grey matter for both techniques are depicted in blue in (2). Voxels of disagreement (i.e. more than 50% difference in the probability of belonging to grey matter) are depicted in (3). Voxels with 50% more probability of belonging to grey matter as per SPM as compared to SIENAx appear in yellow in (4), whereas voxels with 50% more probability of belonging to grey matter as per SIENAx as compared to SPM appear in blue. Striking differences can be observed in the subcortical grey matter nuclei and less so in cortical grey matter inner and outer boundaries.

Registration-based techniques

The brain boundary shift integral (BBSI)[65] and the Structural Image Evaluation, Using Normalization of Atrophy (SIENA)[66] are two image subtraction image analysis methods which rely on initial registration of longitudinal images from the same individual to produce final estimates of variation in volume change (Figure 3). As mentioned before, in both cases reproducibility for brain volume changes is improved compared to that of segmentation-based techniques due to direct calculation of volume changes (in the order of 0.1%-0.2%)[61, 67].

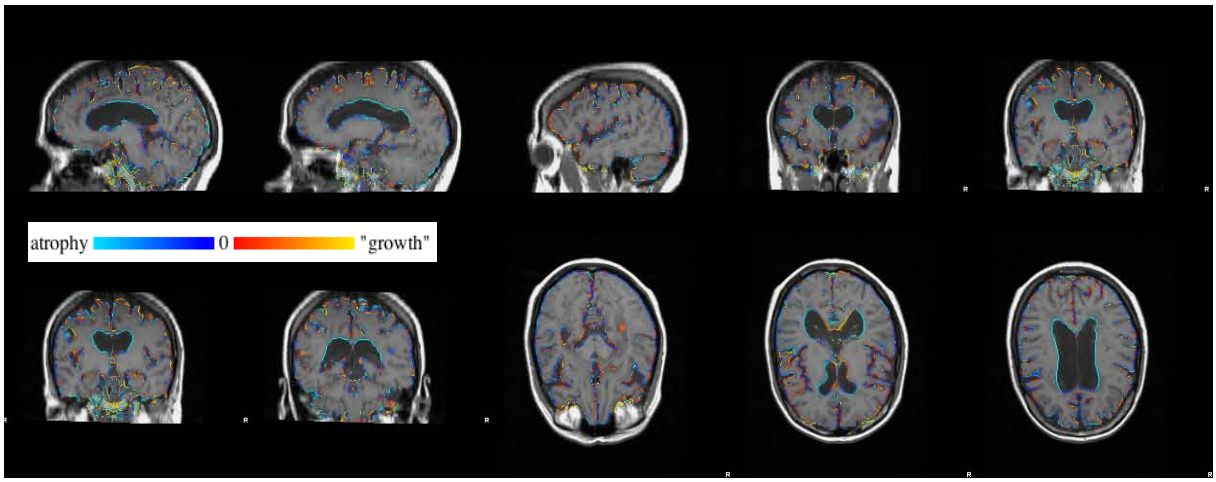

Figure 3. SIENA starts by extracting brain and skull images from the two-timepoint whole-head input data[68]. The two brain images are then aligned to each other[69, 70] (using the skull images to constrain the registration scaling); both brain images are resampled into the space halfway between the two. Next, tissue-type segmentation is carried out[71] in order to find brain/non-brain edge points, and then perpendicular edge displacement (between the two timepoints) is estimated at these edge points. Finally, the mean edge displacement is converted into a (global) estimate of percentage brain volume change between the two timepoints. (Information as provided in SIENA output).

2.3.2 Spectroscopy MR techniques

Magnetic Resonance Spectroscopy (MRS) can be based on a number of chemical nuclei of which the most commonly employed in assessment and research of neurological conditions is the water proton (1H)[72]. Proton MRS allows reliable measurement of a number of metabolites of interest which present a different frequency (these differences are measured in parts per million - ppm) or chemical shift (i.e., position in the spectra) in relation to a standard which is typically the resonance frequency of water[73]: Choline (Cho), Creatine (Cr), Inositol (Ins), N-acetyl-aspartate (NAA) and Glutamate-Glutamine (Glx) as well as other macromolecules, lipids and lactate (Table 1). NAA, which is the second-most-concentrated molecule in the brain after glutamate, can be considered a specific marker of neurons, axons, and dendrites[74] and it is produced in the mitochondria of neurons[75]. Therefore, reduced concentrations of NAA can be interpreted as neuronal (axonal) dysfunction or loss or both. Glutamate and glutamine cannot be readily observed as separate peaks using standard equipment and techniques and, thus, are usually referred as a single mixed peak: Glx. Glutamate is the main excitatory neurotransmitter in the central nervous system; therefore increases in its concentration might be related to increased Glutamate-mediated excitotoxicity[76]. Once released, Glutamate is captured by the astrocytes and converted to Glutamine; Glutamine may be then transferred to the neuron back again to be converted in Glutamate, which will be released under the appropriate stimuli in the so-called Glutamate-Glutamine cycle. Therefore, increased Glutamine can be related to increased astrogliosis[76]. Inositol has been also identified as a relatively specific marker of astroglia (it may participate in the osmoregulatory system in astrocytes) for *in vivo* studies with MRS[77, 78]. This has been reinforced by clinical studies showing an increase in Ins levels in diseases with marked astrogliosis, such as Krabbe leukodystrophy[79]. Elevations of Cho (a main component of cell membranes) are also related to astrogliosis and to increased cell membrane turnover[72]. Finally, the Cr peak represents the added signal of Cr and phosphocreatine, which play an important role in cell metabolism and are present both in neurons as in glial cells[80].

Table 1. Metabolites most commonly measured using spectroscopy techniques in the human brain with chemical shift in ppm (adapted from ref 73).

Metabolite	Short form	Properties	ppm
N-acetyl-aspartate	NAA	Neuronal marker	2.02
Inositol	Ins	Glial marker	3.56
Glutamate-Glutamine	Glx	Excitotoxicity / Glial marker	2.0-2.4
Choline	Cho	Membrane marker	3.22
Creatine	Cr	Cell metabolism	3.03

ppm: parts per million

Proton MRS can be acquired either from specific volumes of interest within the brain or from the brain as a whole without any specific localization[81]. Whole brain MRS is based on the suppression of strong lipid signals from the skull and other non-brain tissues to detect signals from other metabolites, namely NAA, which is restricted to neurons and axons[82]. As other metabolites, like Cr, are also found in other non-brain structures, measurements are not reliable[72]. In practice this technique is restricted to whole brain NAA measurements and is not supported by the manufacturers of clinical MR scanners but would provide a better tool for longitudinal assessments, as registration problems are not an issue as signal comes from the entire brain tissue[83]. Localized MRS can be obtained using a single voxel or a multi-voxel strategy (Table 2). In single voxel acquisitions, spectral information is obtained from a single area of the brain; shorter acquisition times, higher spatial resolution and better spectra quality are counterbalanced by a loss of spatial information in comparison to multi-voxel acquisitions, also known as MRS Imaging (MRSI) or chemical shift imaging (CSI)[72].

Proton MRS can be acquired at short (20-40 ms) or long echo times (135-288 ms). Long echo times allow more robust measurements as spectra appear "cleaner"

(peaks arising from short T2 relaxation time metabolites, such as lipids, are not present) and baseline is well-defined; unfortunately, signal from interesting metabolites, such as Glx, is lost due to its short T2 relaxation time. Short echo time MRS provides information on those metabolites, but makes metabolite quantification a more challenging task due to complex spectra with coarser baselines[72]. Because of good field homogeneity single voxel acquisitions can be obtained easily with short echo times; on the contrary, short echo time MRSI acquisitions are challenging but provide spatially distributed information on a large number of metabolites.

Table 2. Pros and cons of single voxel versus multi-voxel (MRSI) acquisition schemes (adapted from ref 72).

Scheme	Advantages	Limitations
Single voxel	Higher spatial resolution Shorter acquisition times Better spectra quality	Larger voxel sizes Loss of spatial information
MRSI	Smaller voxel sizes Increased spatial information	Worse spatial resolution Longer acquisition times Worse spectra quality

MRSI: Magnetic Resonance Spectroscopy Imaging

MRS acquisitions are usually performed using point resolved spectroscopy (PRESS) or stimulated echo acquisition mode (STEAM) sequences. PRESS allows better signal-to-noise ratios but STEAM is better suited to shorter echo time acquisitions[84].

A common approach to measure metabolite levels is expressing them as ratios to Cr, a metabolite peak that is believed to be stable in many pathological processes[72]. However, assuming that Cr levels are stable may lead to substantial errors[85] and, therefore, absolute quantification of metabolite concentrations should be preferred[86]. A way of measuring absolute metabolite concentrations may be achieved by using an

external reference (commonly referred as a *phantom*) of which metabolite concentrations are known. Probably, the most widely used absolute quantification technique is the Linear Combination Model (LCModel)[87]. The LCModel is a method to measure absolute metabolite concentrations which analyses the in vivo spectrum as a linear combination of spectra from individual metabolites, acquired with the same sequence, contained in a previously prepared solution (model spectrum or *phantom*)[72]. Briefly, absolute quantification is divided in two steps: a) determination of accurate peak areas for the relevant metabolites and b) conversion of peak areas into metabolite concentrations by means of of the calibration procedure[86]. In the application of absolute quantitation methods it is also important to take into account, among other technical aspects, the tissue composition of each voxel (i.e. the relative amounts of CSF, GM and WM), requiring combination of MRSI data with tissue segmentation performed on appropriate 3D T1 sequences[72, 73]. Absolute quantification requires more time and expertise than does relative quantification; in consequence, all additional reference steps must be executed properly if unwanted additional errors are to be avoided (Table 3)[86].

Table 3. Pros and cons of absolute versus intravoxel normalization to Cr quantification schemes (adapted from ref 72).

Method	Advantages	Limitations
Absolute quantification	Data obtained in mmol	Sensitive to: 1. partial volume 2. calibration to phantom 3. scanner stability 4. changes in T1/T2
Creatine ratios	Not sensitive to: 1. edema 2. changes in T1/T2	Changes in Cr levels

2.3.3 Atrophy and Spectroscopy findings in healthy subjects: effect of age

Biological ageing has an impact on both brain atrophy and spectroscopy findings. Therefore, any attempt to gauge the effect of pathology on such findings should take into account, whenever possible, age as a covariate. A better understanding of brain ageing is thus warranted.

Global brain **volume loss** occurs at a pace of 0.18%-0.33% per annum[88, 89]. Brain volume shrinkage may differ with age, so that elder individuals may display an acceleration of that rate[88, 89]. Decline rates appear to be different for GM (-0.1%) and WM (0.2%)[90]. GM volume loss appears to be constant and linear in adult life (starting at the age of 20) whereas WM volume loss only occurring from the age of 40 onwards[91]; before that age, WM seems to be stable or with a slight increase[90, 92]. Gender differences do not seem to be that clear-cut, although larger WM fractions have been reported in females, and steeper declines in GM volumes in males[90]. It is of note that in healthy adults longitudinal changes in brain volume are not evenly distributed; although brain volume loss is diffuse, some brain regions seem to be more affected by this process (caudate, cerebellum, hippocampus, tertiary association cortices) than others (fusiform cortex, entorhinal cortex, primary visual cortex and the pons)[91]. The effect of aging is also more intensely felt in the deep WM tracts connecting the GM areas more affected by the aging process[88]. Finally, the effect of age on decline rates does not seem to be similar across areas[91].

Spectroscopy studies of normal ageing have shown significant decline in relevant brain metabolites[88]. A large number of cross-sectional studies have revealed decreased NAA levels with increasing age in different brain areas[93-96]. Although Cr and Cho levels have been reported to be stable, some studies have revealed changes with ageing, emphasising the need to use absolute metabolite concentrations to avoid spurious results[97, 98]. On the other hand, longitudinal studies have yielded conflicting results, as some studies have found stability over time of NAA levels,

whereas others have found significant decreases of NAA levels with age at a similar rate in women as in men[99, 100]; the low reproducibility of spectroscopy studies, which is a very important limitation for multicentre studies in large samples, may be the reason for this[101].

2.4 MR in Primary Progressive Multiple Sclerosis

2.4.1 Early studies – conventional MRI

The earliest studies using MRI in PPMS[102, 103] immediately reached the conclusion that patients with PPMS in spite of higher levels of disability "*had surprisingly few lesions*" [102]. These studies also underscored differences in the dynamics between the progressive forms of MS; patients with PPMS, as compared to patients with SPMS had a lower rate of new lesion formation and a lower frequency of lesion enhancement in new lesions[103]. The MAGNIMS (Magnetic Resonance in Multiple Sclerosis) network has greatly contributed to the understanding of the evolution of conventional MRI features of PPMS through a longitudinal study of a well-characterised cohort of patients with PPMS[38, 104-107]. The baseline description of this PPMS cohort[38] confirmed the previous findings in the sense that the PPMS group had lower lesion volumes (both on T2- and T1-weighted MRI sequences) than a reference SPMS group; this finding was further extended to indicate that PPMS patients had also a lower number of lesions in the spinal cord as compared to patients with SPMS. The absence of a significant correlation between lesion volume and disability (which was indeed observed for brain and spinal cord atrophy – see below), raised the issue of neurodegeneration as a main pathological process and responsible for disability in PPMS as opposed to the role of focal lesions. Interestingly, patients presenting clinically with a spinal cord syndrome were found to have lower brain lesion volumes as compared to those with non-spinal cord

presentations. This cohort was later on reassessed at one[104], two[105], five[106] and ten[107] years. The main conclusions of these studies can be summarized as follows:

1. In spite of lower lesion volumes as compared to MS relapsing forms, statistically significant changes did occur, both in T2- and T1-weighted lesion volumes in periods as short as one year; this would make possible the use of lesion volumes as MRI outcomes in clinical trials.
2. Changes in T2 lesion volume and the number of new lesions over the first two years of follow-up were found to be independently predictive of clinical outcome at five years.
3. However, lesion-related parameters were not found to significantly predict outcome at ten years, in contrast to atrophy measures (see below).

To further blur the boundaries between PPMS and MS relapsing forms in terms of the impact of lesion-related parameters, a study[108] performed on a cohort of early PPMS (recruited in the first five years of disease duration) showed that enhancing lesions were not infrequent, as up to 40% of patients showed brain enhancing lesions, and such patients had worse clinical and MRI parameters. Even though frequency was lower to that reported in early RRMS[109], duration of enhancement was very similar to that observed in patients with RRMS, as of the 25 enhancing lesions at baseline, five were enhancing one month later and only one showed enhancement at 2 months. In contrast, spinal cord enhancing lesions were found to be rare (7%). Along these lines, a subanalysis of the 10-year follow-up MAGNIMS cohort has also indicated that lesion location in motor and associative pathways is an important contributor to the progression of disability[110, 111].

In summary, the unifying concept of MS appears to be also plausible according to conventional MRI data, as the differences between relapsing MS and PPMS seem to be quantitative rather than qualitative[27].

2.4.2 Non-conventional MR

Non-conventional MR is a rather loose term that refers to a set of MR techniques, which are not usually applied in clinical practice, and which tend to need specific sequences and pre and post-processing of images before a final parameter is obtained. Techniques that are considered as non-conventional MR include: atrophy measurements, MRS, magnetization transfer imaging (MTI), diffusion tensor imaging (DTI) and functional MRI (fMRI). In recent years, atrophy measurements are becoming widely used and may well now be considered as conventional, as post-processing is now fully automated and no specific sequences are needed.

Atrophy measures.

In the baseline analysis of the longitudinal MAGNIMS cohort[38], no significant difference was found in the six-slice measure of brain volume between the PPMS and the SPMS groups. However, measurement of the spinal cord cross-sectional area revealed that the SPMS group had a significantly smaller area than either the PPMS and the Transitional Progressive Multiple Sclerosis (TPMS) group (a group with a predominantly progressive phenotype but which may have presented relapse activity). Both measures of atrophy displayed clinical correlations, albeit moderately. In the one year follow-up of this cohort[104], statistically significant decreases in brain volume were already observed but not in spinal cord area; no correlation between such changes and clinical changes was observed. However, the follow-up at five years[106] showed that brain volume and spinal cord area changes in the first two years were independently predictive of disability at five years, together with lesion-related parameters. Interestingly enough, in the 10 year assessment of this cohort[107] brain volume was the only MRI metric change in the first two years to independently predict clinical outcome at 10 years. Taken together these results may indicate that brain volume and spinal cord measurements can be taken as predictive of clinical outcome especially in the long term, and that their predictive power adds up to the more short term effect by the lesion-related parameters. Unfortunately, none of the

clinical trials in which brain volume was considered as a surrogate outcome of efficacy showed any effect of the drugs tested on atrophy development[36, 37, 40].

Other non-conventional techniques: MRS, MTI, DTI, fMRI.

Overall[112], these techniques have been able to show that damage that goes undetected to conventional MRI techniques do occur in the normal appearing white and grey matter of people with PPMS. Finally, cortical adaptive responses have been observed in PPMS using fMRI, indicating that clinical disability may not be a direct consequence of tissue damage and loss, and that the neuroplastic capacities of the brain and spinal cord may play a role in adapting, at least up to a certain level, to such damage[112].

3. WORKING HYPOTHESIS

Disability in patients with PPMS is associated not only with lesion-related MRI parameters but also with other parameters obtained with the use of MR techniques investigating the normal-appearing tissue. Such associations can be detected in patients early in their disease course, where EDSS changes have not reached a plateau in their bimodal distribution[20]. Brain volume and MRS measurements are useful techniques in this regard, and will show significant correlations with clinical parameters as well as changes in the short term, making them amenable to use in clinical practice as well as making their inclusion in clinical trials worth of further investigation, when dealing with patients with the PPMS phenotype.

4. OBJECTIVES

ATROPHY STUDIES

1. To compare brain tissue fractions (whole brain, grey and white matter fractions) from a cohort of patients with early PPMS with those from a control group matched by age and gender
2. To investigate the association of brain tissue fractions with lesion-related MRI parameters in this cohort
3. To investigate the association of brain tissue fractions with clinical parameters in this cohort
4. To asses the degree of change of brain tissue fractions over the short term (one year of follow-up) in this cohort
5. To investigate clinical and MRI predictors of brain tissue fractions changes in the short term

MRSI STUDIES

1. To compare the concentration of brain tissue metabolites obtained with short-echo MRSI - Choline, Creatine, Inositol, N-acetyl-aspartate and Glutamate-Glutamine - from a cohort of patients with early PPMS with those from a control group matched by age and gender
2. To investigate the association of brain tissue metabolites with lesion-related MRI parameters in this cohort
3. To investigate the association of brain tissue metabolites with clinical parameters in this cohort
4. To asses the degree of change of brain tissue metabolites over the short term (one year of follow-up) in this cohort
5. To investigate clinical and MRI predictors of brain tissue metabolite changes in the short term

5. MATERIAL AND METHODS

5. 1 Patients, controls and clinical assessments

Inclusion criteria for patients were as follows: fulfilment of the PPMS diagnostic criteria[32] (definite or probable) and a history of clinical progression of less than five years. At baseline, 43 consecutive patients with PPMS in the early clinical stages of disease evolution and 45 control subjects were recruited at the National Hospital for Neurology and Neurosurgery, Queen Square, London. MRSI and atrophy studies were usable on 41/42 patients only (one patient did not attend for MRSI / atrophy and MRSI data from another patient could not be analysed due to technical issues) and on 44 controls due to one technical failure. At follow-up, twelve months later, 31 patients from the original cohort were reassessed for atrophy (6 patients had missed their one year appointment but still on follow-up, 5 patients were already lost to follow-up by that time-point, and 1 patient MRI scans could not be analysed due to a technical failure) and 30 for MRSI (as one of the 31 patients did not have MRSI at baseline due to a technical failure). Longitudinal analyses are based on patient-only data.

All patients underwent conventional neurological assessment at baseline and were scored on the EDSS[113] and MSFC[114] at baseline. Z scores for the MSFC subtests (nine-hole peg test –NHPT-; timed walk test –TWT-; paced auditory serial addition test -PASAT-) were obtained by averaging all trials for each subtest, and calculated using the preferred method (i.e. using our own sample baseline values as a reference to derive mean and standard deviation)[115]. Z scores were averaged to obtain a single MSFC score for each patient. The formula for creating the MSFC score is presented in the *MSFC Administration and Scoring Manual*[116]. The joint ethics committee of the National Hospital for Neurology and Neurosurgery and the Institute of Neurology (London) approved the protocol prior to study initiation. All subjects gave written informed consent before being included in the study.

5.2 MR methods

5.2.1 Scan acquisition

All images were acquired using a 1.5 T GE Signa scanner (General Electric, Milwaukee, USA). No major hardware upgrades were carried out on the scanner, and weekly quality assurance sessions guaranteed the stability of measurements throughout the duration of the study.

For atrophy studies, a 3D inversion-prepared fast spoiled gradient recall (3DFSPGR) sequence was acquired (124 contiguous axial slices, echo time -TE- 4.2 ms, repetition time -TR- 13.3 ms, inversion time 450 ms, number of excitations -NEX- 1, field of view -FOV- 300 x 225 mm over an image matrix of 256 x 160 [interpolated to a 256 x 256 reconstructed matrix for a final X-Y in-plane resolution of 1.17 x 1.17 mm], slice thickness -ST- 1.5 mm).

For MRS studies, MRSI data were acquired from a volume located superior to the roof of the lateral ventricles (Figure 4) using a PRESS localization sequence (TE 30 ms, TR 3000 ms, NEX 1, 24 x 24 phase encodes over a FOV of 30 x 30 cm, spectral width 2500 Hz, number of points 2048, ST 15 mm, nominal voxel volume 2.3 ml) with outer-volume suppression bands. The size of PRESS-selected volume varied between subjects according to head size and, as a consequence, the dimensions of the grid of voxels (Figure 5) were variable among individuals. At baseline, a total of 5005 voxels were obtained; in patients, the range of voxels per grid was 36 to 70 and the total number of voxels obtained was 2371; in control subjects, the range of voxels per grid was 42 to 70 and the total of voxels obtained was 2634. For the longitudinal analyses a total of 3537 voxels were obtained (only patients were scanned at follow-up); 1777 corresponded to patient baseline voxels, where the

range of voxels per grid was 42 to 70; 1760 corresponded to patient follow-up voxels, where the range of voxels per grid was 42 to 80.

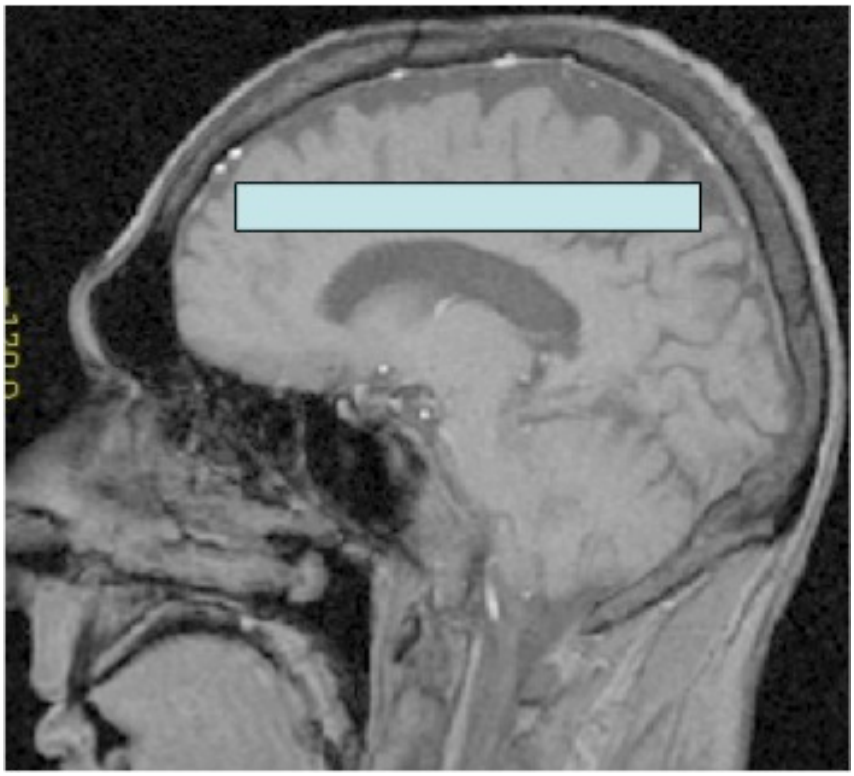

Figure 4. Magnetic Resonance Spectroscopy Imaging data were acquired from a volume superior to the roof of the lateral ventricles.

Two other sets of sequences were acquired: a dual spin echo sequence (28 contiguous slices, TE 30/80 ms, TR 1720 ms, NEX 0.75, ST 5 mm); and a T1 weighted spin echo sequence (28 contiguous axial slices, TE 20 ms, TR 540 ms, NEX 1, flip angle 90º, ST 5 mm), acquired before and 5 minutes after intravenous administration of triple dose Gd (0.6 ml/kg of body weight; Magnevist, Schering, Germany). For the sake of patients comfort, scan sessions were split into two, T1 Gd-enhanced scans were acquired in a separate session; the mean separation between sessions was 20.4 days at baseline for the baseline atrophy dataset (median: 13; interquartile range: 7 - 25), 19.5 days at baseline for the MRSI baseline dataset (median: 12.5; interquartile range: 7 - 24) and 14.8 days at baseline for the atrophy and MRSI one year follow-up dataset (median: 7; interquartile range: 7 to

24). The 3DFSPGR and MRSI sequences were acquired again one year later in patients only (mean time between acquisitions: 12.2 months; interquartile range: 11.4 to 13.1).

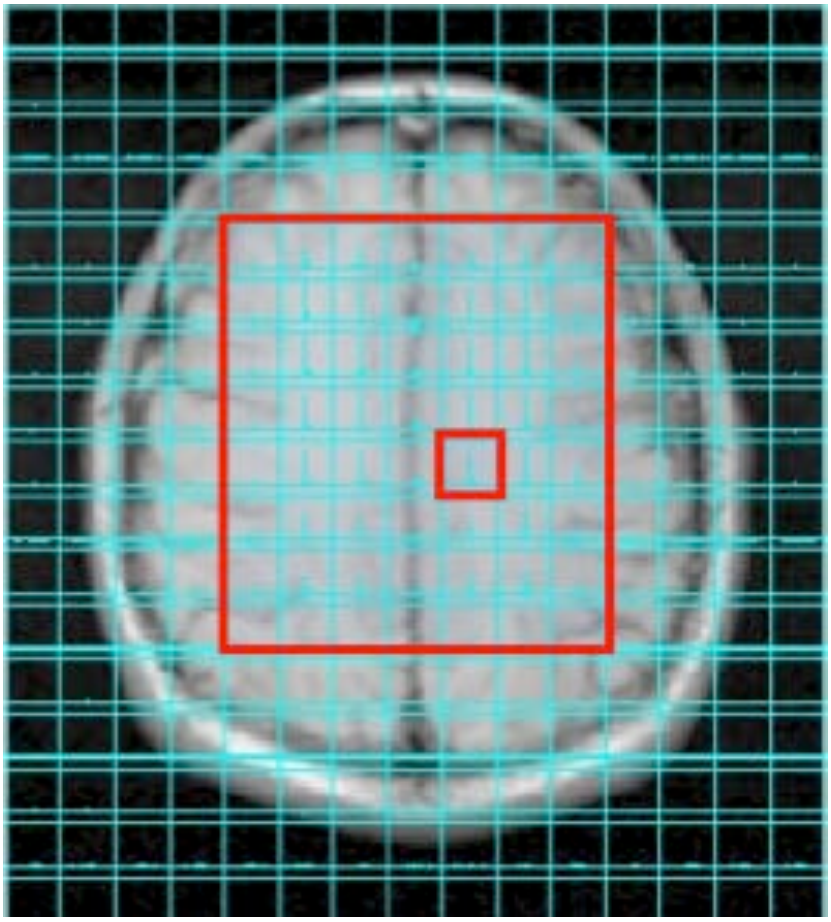

Figure 5. Grid of voxels from which Magnetic Resonance Spectroscopy Imaging data were acquired overlaid on an axial T1-weighted image. A central voxel is singled out within the grid. At baseline, 5005 voxels from patients and controls were obtained; at follow-up the number of voxels obtained was 3537

5.2.2 Image analysis

Lesion contouring and brain segmentation. Images were segmented in to WM, GM and CSF using SPM99 and following previously described methodology[60] (Figure 6). Visual inspection of baseline SPM99 outputs enabled us to detect one segmentation

failure and data from this patient were discarded. Lesion contouring was performed on 3DFSPGR and on proton density (PD) weighted images, and Gd-enhancing lesion volumes were determined using a semiautomatic local thresholding contour technique (Dispimage, DL Plummer, University College London, London) yielding PD and enhancing lesion volumes respectively, and blindly to clinical data. The intra-rater intra-class correlation coefficient for 3DFSPGR lesion contouring was 0.995. Using in-house software, the lesion contours derived from 3DFSPGR images were subtracted from WM, GM and CSF masks, yielding four mutually exclusive tissue masks with their associated volumes in ml. Volumes were estimated after truncation of the spinal cord, with a caudal cut-off point defined as the most cranial slice of cord not-containing cerebellum. Total intracranial volume (TIV) was calculated as WM + GM + CSF + lesion mask volumes. BPF was calculated as (WM + GM + lesion mask volumes) / TIV; WMF as (WM + lesion mask volumes) / TIV; and GMF as GM volume/ TIV. The impact of lesion masks on brain tissue fractions is known to be small (lesion fraction in our population is of 0.8% of total intracranial volume) but counting all lesions as WM would further reduce this miscalculation (all lesions detected on the 3DFSPGR sequence were in WM)[60]. Brain atrophy was also estimated on 3DFSPGR images from baseline and 1-year scans using SIENA version 2.2 (available at http://www.fmrib.ox.ac.uk/analysis/research/siena/) to obtain a Parenchymal Brain Volume Change (PBVC) estimate.

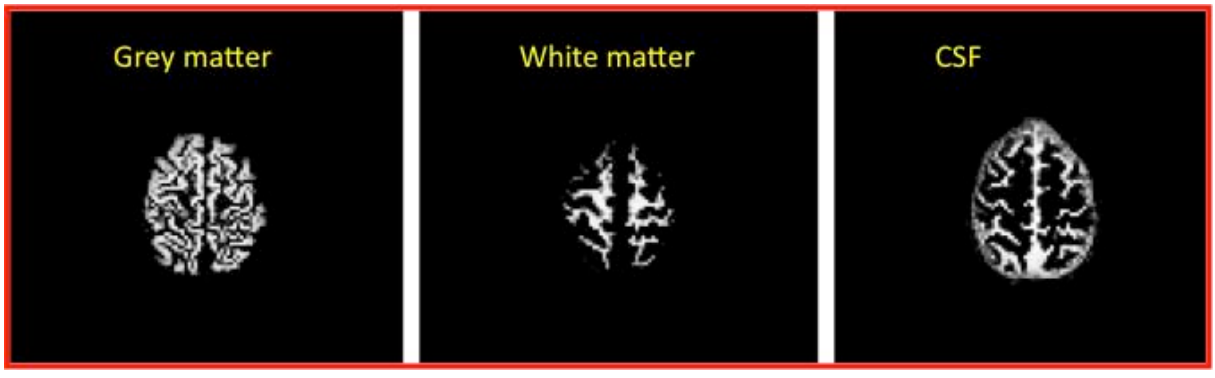

Figure 6. Figure showing SPM99 output. Three mutually exclusive masks are generated corresponding to grey matter (left), white matter (central), and CSF (right). The lesion mask is then subtracted from these, generating a fourth mutually exclusive mask.

MRSI analysis. MRSI data obtained from individual voxels was processed using the LCModel[87] (Figure 7) to fit individual spectra from each voxel to a combination of in vitro spectra. Metabolite concentrations and Cramer Rao minimum variance bounds (CRMVB) were estimated for five metabolites: Cho, Cr, Ins, total N-acetyl-aspartate (tNAA) and Glx; tNAA refers to the sum of NAA and N-acetyl-aspartyl-glutamate.

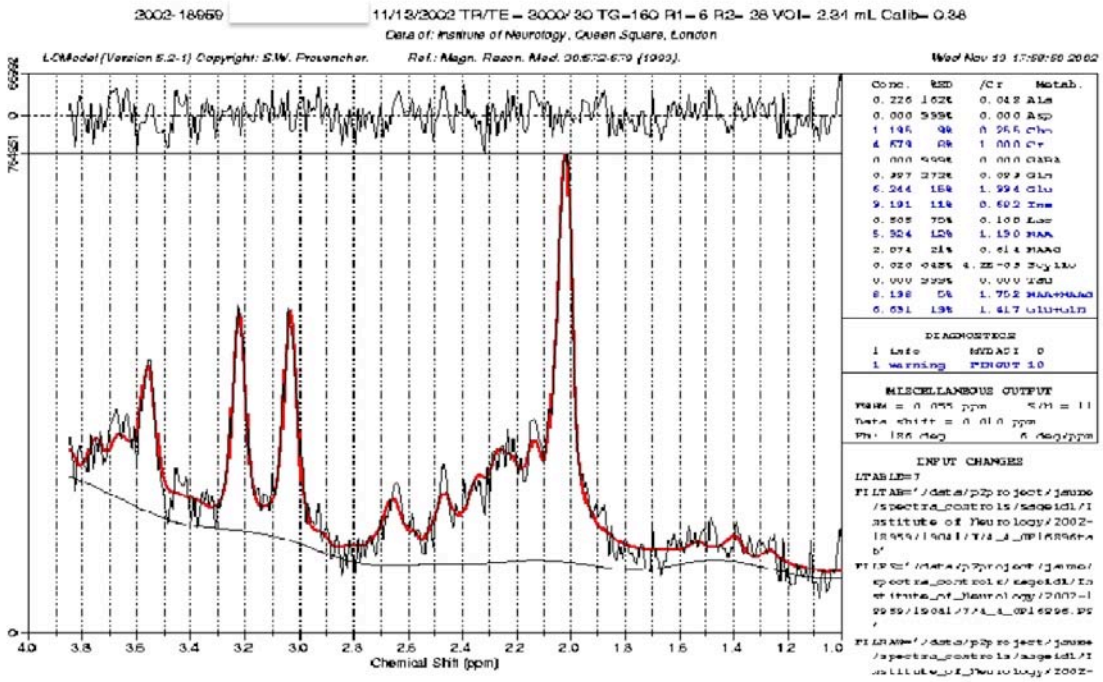

Figure 7. Figure showing LCModel output with fitting of the different peaks of the spectrum from a single voxel of a subject of the present sample. Metabolite concentrations are presented on the top right part of the output together with creatine ratios (not used in the present study).

Cross-sectional MRSI analysis at baseline. The total number of voxels obtained at baseline was 5005 (2634 from controls and 2371 from patients). No k-space filtering was applied during processing, so a voxel volume equal to the nominal grid size was assumed. To correct for the imperfect excitation profile a quantitative measure of radiofrequency excitation for every voxel was obtained[117]. Using a 90% cut-off point, 2279 voxels were still retained. This exclusion criterion eliminated voxels from the outer layers of the grid, which may artefactually yield lower metabolite concentration

values and usually display higher CRMVBs after LCModel fitting[117]. Voxels with a CRMVB for any given metabolite two standard deviations above the mean of CRMVBs for that metabolite, or with a content of less than 80% in GM plus WM were also excluded. Finally, voxels that contained a significant amount of lesional tissue were also discarded (to achieve this, we set up a stringent criteria of a maximum of 1% of lesion fraction). All GM included in the grid was cortical GM. Of the 1620 voxels remaining, those containing more than 60% of WM (1115 voxels: 724 from controls and 391 from patients) were classified as NAWM and those containing more than 60% of cortical GM (154 voxels: 113 from controls and 41 from patients) were classified as cortical GM. This classification is the same as that which was successfully applied in a previous study of a cohort with RRMS[118]. This means that a grand total of 351 initially retained voxels was discarded because of mixed tissue contents (i.e. less than 60% of either GM or WM in the voxel). The differences in the final number of voxels available for analysis in patients and controls may relate to different factors: a larger number of voxels available from outset in controls than in patients (2634 versus 2371 voxels) and greater amount of CSF in voxels from patients (13.41% versus 9.3% of mean CSF content per voxel) reflecting relatively atrophic brains in MS when compared with control subjects. A mean concentration for a given metabolite in cortical GM and NAWM voxels was obtained for each patient and control and entered in to the statistical modelling. Finally, 39 controls and 24 patients yielded usable cortical GM voxels, while 44 controls and 37 patients yielded usable NAWM voxels.

Longitudinal MRSI analysis. Longitudinal analyses are based on patient-only data. The total number of voxels obtained for the longitudinal analysis was 3537 voxels (1777 from baseline examinations and 1760 from follow-up examinations). The MRSI analysis follows a similar methodology than that used for baseline examinations. Using a 90% radiofrequency excitation cut-off point, 1614 voxels were still retained. Voxels with a CRMVB for any given metabolite two standard deviations above the mean of CRMVBs for that metabolite, or with a content of less than 80% in GM plus WM were also excluded. Finally, voxels that contained a significant amount of lesional tissue (<1% lesion fraction) were also discarded. After, applying CRMVB and

CSF and lesions tissue contents cut-offs 769 voxels remained. All GM included in the grid was cortical GM. A less stringent cut-off for GM and WM content was used in baseline and follow-up analyses (60% vs 50%) due to extreme voxel drop out for the follow-up sample. Therefore, voxels containing more than 50% of WM (587 voxels: 322 from baseline and 265 from follow-up) were classified as NAWM and those containing more than 50% of cortical GM (128 voxels: 70 from baseline and 58 from follow-up) were classified as cortical GM. This means that a total of 54 initially retained voxels was discarded because of mixed tissue contents. A mean concentration for a given metabolite in cortical GM and NAWM voxels was obtained for each patient and entered in to the statistical modelling. Finally, 21 pairs of baseline / follow-up examinations yielded, concomitantly, usable cortical GM voxels, while 24 pairs of baseline / follow-up examinations yielded, concomitantly, usable NAWM voxels to be introduced in the longitudinal analysis.

5.3 Statistical analysis

Statistical analysis was performed using SPSS v10 and v11.5 (Chicago, IL, USA).

For the baseline atrophy dataset, a general linear model analysis was used to investigate the effect of MS on BPF, WMF and GMF; gender and disease status (control or MS) were included as fixed factors, age as a continuous covariate, and an interaction factor between gender and age was also introduced into the model. Pearson correlation coefficients were used to assess the presence of linear associations between the tissue fractions (BPF, WMF, GMF) and clinical and radiological variables, except for EDSS when Spearman Rank Correlation coefficients were calculated. A general linear model analysis was used to investigate the effect of onset type of PPMS (cord versus non-cord) on BPF, WMF, and GMF; age was included as a covariate and gender and onset type as fixed factors. Significance values for all correlation coefficients are reported without correction for multiple comparisons to avoid type II errors[119].

For the one year follow-up atrophy dataset, a paired samples T-test was performed to detect statistically significant differences between baseline and one year estimates of atrophy (BPF, GMF and WMF) and a one sample T-test for PBVC. Percentage changes in tissue fractions were obtained by subtracting the baseline from the one year follow-up estimates and dividing by the baseline values, then multiplying by 100. Pearson correlation coefficients were used to assess the presence of linear associations between PBVC, the percentage change in tissue fractions (BPF, GMF and WMF) and clinical and radiological variables, except for EDSS when Spearman Rank Correlation coefficients were calculated. Significance values for all correlation coefficients are reported without correction for multiple comparisons to avoid type II errors[119]. Stepwise linear regression was performed with PBVC, and the percentage change in tissue fractions (BPF, GMF and WMF) as dependent variables against three sets of independent variables: clinical (age, disease duration, EDSS, MSFC), radiological (age, disease duration, number of Gd-enhancing lesions, proton density lesion volume) and combined (age, disease duration, EDSS, MSFC, number of Gd-enhancing lesions, proton density lesion volume).

For the MRSI baseline dataset a general linear model analysis was used to determine the effect of MS on brain metabolite concentrations while allowing for age, gender, voxel tissue contents and potential partial volume effects associated with brain atrophy. Gender and disease status (control or MS) were included as a categorical variable; age, brain parenchymal volume (in ml), CSF and cortical GM content (in percentage) for NAWM voxels, and CSF and NAWM content (in percentage) for cortical GM voxels were included as continuous covariates. Spearman correlation coefficients were used to assess the presence of linear associations between metabolite concentrations in cortical GM and NAWM and both clinical (EDSS and MSFC) and other radiological variables (brain tissue fractional volumes and lesion volumes). Significance values for Spearman coefficients were not corrected for multiple comparisons to minimise the risk of type II errors[119].

For the MRSI one-year follow-up dataset paired statistics (parametric t-tests and Wilcoxon signed ranks tests) on baseline and follow-up metabolite concentrations for the different tissue types were performed. After that, metabolite change variables (baseline minus follow-up) were created and, NAWM, CSF and cortical GM content (in percentage) for NAWM voxels, and NAWM, CSF and cortical GM content (in percentage) for cortical GM voxels were centered on their means. A general linear model analysis with change variables as dependent variables was then used to detect significant differences after adjusting for mean-centered tissue concentrations.

6. ATROPHY FINDINGS

6.1 Baseline

Forty-three patients with early PPMS and 45 control subjects were included in this study. Clinical and demographical features of both samples are provided in Table 4. Gender ratio for patients with PPMS was 1.2 (male:female), median age at scanning was 46 years and median EDSS was 4.5; all of them compatible with a typical PPMS sample.

Table 4. Clinical and demographic features of patients and controls.

	Controls (n=45)	Patients (n= 43)
Sex ratio (male/female)	51% / 49%	55% / 45%
Age at scanning*	38.5 (23 to 67)	46 (22 to 65)
Disease duration (years)**	-	3.32 (2 to 5)
EDSS*	-	4.5 (3 to 7)
MSFC**	-	-0.318 (-5.63 to 1.13)
NHPT Z score**	-	0 (-2.28 to 2.16)
TWT Z score**	-	0.955 (-0.46 to 13.7)
PASAT Z score**	-	0 (-2.88 to 1.26)

*median (range); **mean (range); EDSS: Expanded Disability Status Scale; MSFC: Multiple Sclerosis Functional Composite; NHPT: nine-hole peg test; TWT: Timed walk test; PASAT: Paced auditory serial addition test.

Comparison of brain tissue fractions between PPMS and control subjects

After allowing for age and gender effects, there were statistically significant differences between patients and control subjects in BPF, WMF and GMF ($p<0.001$) with a percentage change relative to control subjects of -4.4%, -6.2% and -3.5% respectively (Table 5).

Table 5. Radiological features of patients and controls.

	Controls (n=45)	Patients[1]
BPF[2]	0.83 (0.70 to 0.87)	0.79 (0.70 to 0.86)
WMF[2]	0.28 (0.22 to 0.31)	0.26 (0.20 to 0.30)
GMF[2]	0.55 (0.48 to 0.59)	0.52 (0.48 to 0.58)
Number of Gd+ lesions	-	1.07 (0 to 9)
Volume of Gd+ lesions[3]	-	0.14 (0 to 0.58)
PD lesion volume[3]	-	14.62 (0.19 to 96.83)

All values presented: mean (range); [1](n=42 for PD and Gd; n=41 for BPF, WMF, GMF); [2](all differences in patients vs controls significant at p<0.001 level); [3]lesion volumes in ml; BPF: brain parenchymal fraction; WMF: white matter fraction; GMF: grey matter fraction; Gd+: gadolinium positive; PD: proton density.

Scatter plots of BPF, WMF and GMF against age in patients with PPMS and controls show lower values of BPF, WMF and GMF for patients across the entire age range (Figure 8). Age-dependent behaviour of GMF and WMF are compatible with what has been described in the literature, mostly in the healthy control group[88, 90].

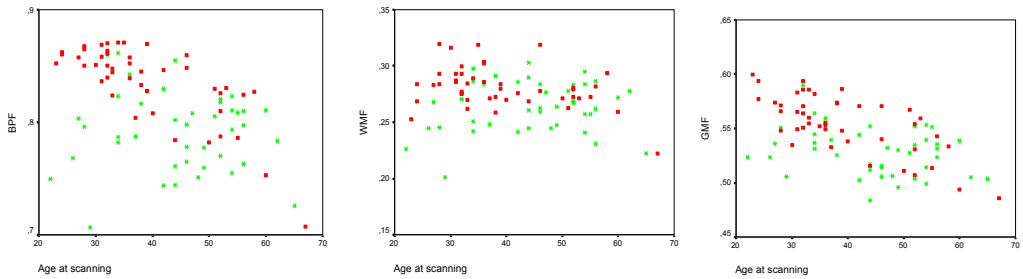

Figure 8. Brain parenchymal fraction (BPF), white matter fraction (WMF) and grey matter fraction (GMF) plotted against age for patients with primary progressive multiple sclerosis (green crosses) and healthy controls (red full squares).

Radiological associations of atrophy measures

Statistically significant correlations were found between PD lesion volume and BPF and WMF (Table 6). This correlation was non-significant for GMF. Significant correlations were also observed between Gd-enhancing lesion volume and number and WMF (only a trend for BPF with Gd-enhancing lesion numbers); no statistically significant correlations were observed between GMF and Gd-enhancing lesion number and volume.

Table 6. Correlations between BPF, WMF, GMF and lesion parameters.

		r	p
BPF	vs Enhancing lesion numbers	-0.308	0.053
	vs Enhancing lesion volumes	-0.256	0.111
	vs PD-weighted lesion volume	-0.529	<0.001
WMF	vs Enhancing lesion numbers	-0.389	0.013
	vs Enhancing lesion volumes	-0.315	0.048
	vs PD-weighted lesion volume	-0.583	<0.001
GMF	vs Enhancing lesion numbers	-0.090	0.582
	vs Enhancing lesion volumes	-0.084	0.606
	vs PD-weighted lesion volume	-0.249	0.121

BPF: brain parenchymal fraction; WMF: white matter fraction; GMF: grey matter fraction; PD: proton density.

To obtain a more accurate estimate of the strength of this relationship, a further regression analysis was performed between PD lesion volume and WMF and GMF (corrected for age using our own control subject population data). The regression equations obtained with this analysis (age-corrected WMF = 0.224 – 0.000411 x lesion volume; non significant results for age-corrected GMF) would better indicate the effect, in isolation, of PD lesion volume on atrophy measures (Figure 9).

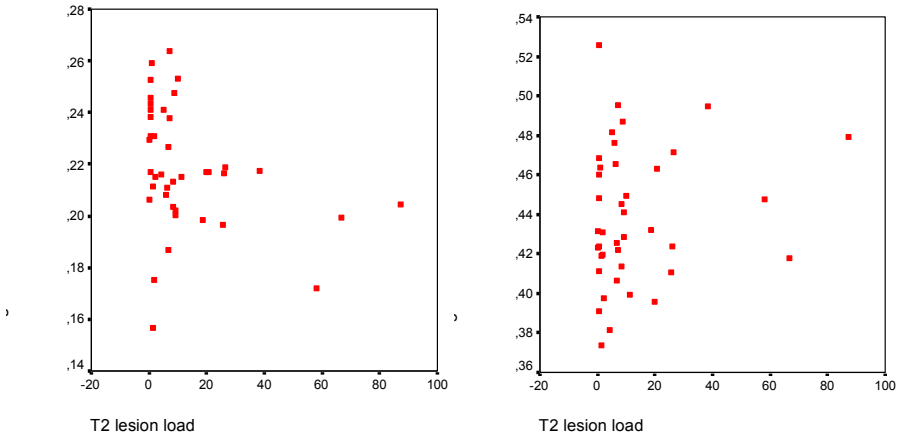

Figure 9. Age-corrected white matter fraction (WMF) -left- and grey matter fraction (GMF) -right- against proton density lesion volume (in ml) in patients with primary progressive multiple sclerosis.

Clinical associations of atrophy measures

None of the atrophy measures correlated with disease duration (Table 7). BPF and WMF showed moderate correlations with EDSS and MSFC scores, while GMF correlated moderately with MSFC alone. All three MSFC subtests (PASAT, TWT, NHPT) were moderately correlated with BPF. WMF and GMF correlated significantly with the Z scores on the NHPT, but only WMF correlated with the Z scores on the TWT; trends for a correlation with the Z scores on the PASAT were seen for GMF and WMF.

After allowing for age and gender effects, the only significant difference between cord and non-cord presentations was that patients with a non-cord presentation had smaller WMFs (-8.2% of fractional values; p=0.024) than those with a cord presentation.

Table 7. Correlations between BPF, WMF, GMF and clinical variables.

		r	p
BPF	vs disease duration	-0.155	0.334
	vs EDSS	-0.469	0.002
	vs MSFC	0.518	0.001
	vs NHPT	0.577	<0.001
	vs TWT	-0.361	0.021
	vs PASAT	0.361	0.020
WMF	vs disease duration	-0.089	0.581
	vs EDSS	-0.532	<0.001
	vs MSFC	0.483	0.001
	vs NHPT	0.585	<0.001
	vs TWT	-0.337	0.031
	vs PASAT	0.284	0.072
GMF	vs disease duration	-0.159	0.321
	vs EDSS	-0.195	0.223
	vs MSFC	0.337	0.031
	vs NHPT	0.325	0.038
	vs TWT	-0.234	0.141
	vs PASAT	0.289	0.067

BPF: brain parenchymal fraction; WMF: white matter fraction; GMF: grey matter fraction; EDSS: Expanded Disability Status Scale; MSFC: Multiple Sclerosis Functional Composite; NHPT: nine-hole peg test; TWT: timed walk test; PASAT: paced auditory serial addition test.

6.2 One year follow-up

Thirty-one patients with PPMS within five years of disease onset were recruited at the National Hospital for Neurology and Neurosurgery, Queen Square, London for this study. As mentioned in the material and methods section, they were all part of the cohort scanned at baseline in the previous study. The 31 patients (Table 8) with clinically early PPMS (less than five years of disease duration) had a mean follow-up time of 12.2 months (interquartile range: 11.4 to 13.1).

Table 8. Baseline clinical, demographic and radiological features of patients.

	Patients (n= 31)
Sex ratio (male/female)	58% / 42%
Age at scanning*	46 (26 to 62)
Disease duration (years)*	3.0 (2 to 5)
EDSS*	4.5 (3.5 to 7)
MSFC**	-0.316 (1.44)
Brain parenchymal fraction**	0.796 (0.035)
White matter fraction**	0.266 (0.022)
Grey matter fraction**	0.529 (0.023)
Number of Gd+ lesions**	0.96 (1.44)
Patients with Gd+ lesions	48.4 %
PD lesion volume**,***	26.01 (22.97)

*median (range); **mean (standard deviation); ***lesion volume in ml; EDSS: Expanded Disability Status Scale; MSFC: Multiple Sclerosis Functional Composite; Gd+: gadolinium positive; PD: proton density.

Evolution of brain atrophy (Table 9, Figures 10 and 11)

Using the SPM-based segmentation method statistically significant decreases ($p<0.001$) were observed in both BPF (mean -1.03%; standard deviation: 1.3%) and GMF (mean -1.50%; standard deviation: 1.6), whereas WMF did not change significantly (-0.07%; $p=0.749$). Using SIENAv2.2 a PBVC of -0.63% (standard deviation: 1.05) was observed ($p=0.002$).

Table 9. Values of brain parenchymal fraction, white matter fraction and grey matter fraction obtained with SPM and PBVC obtained with SIENA

	Baseline	12 months	p
Brain parenchymal fraction*	0.796 (0.035)	0.787 (0.038)	<0.001
White matter fraction*	0.266 (0.022)	0.266 (0.022)	0.749
Grey matter fraction*	0.529 (0.023)	0.521 (0.025)	<0.001
PBVC*, **	-	-0.636 (1.05)	0.002

* mean (standard deviation); ** values for PBVC represent percentage changes from baseline examination. PVBC: percentage brain volume change.

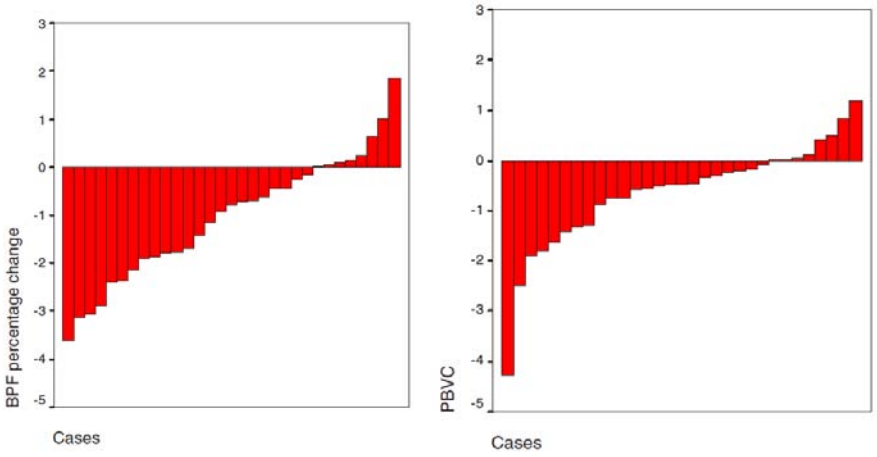

Figure 10. Bar graphs displaying, for each case, percentage brain volume change (PBVC) obtained with SIENAv2.2 and percentage changes in brain parenchymal fraction (BPF) obtained with SPM.

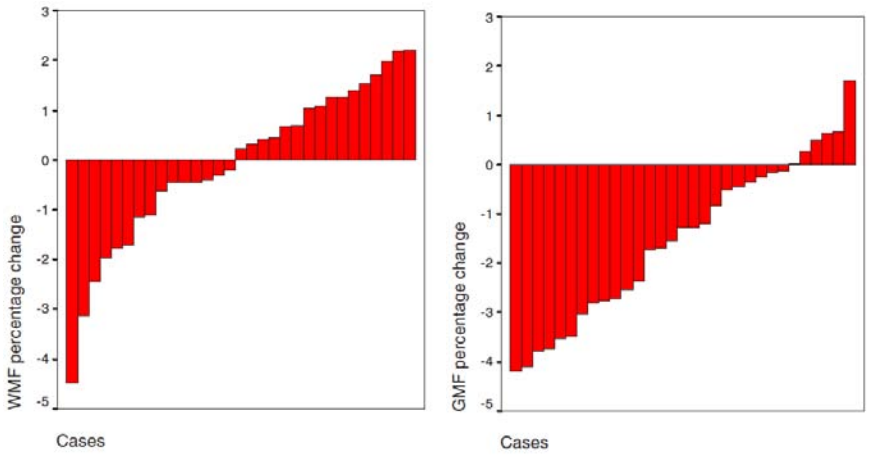

Figure 11. Bar graphs displaying, for each case, percentage changes in white matter fraction (WMF) and grey matter fraction (GMF) obtained with SPM.

Brain atrophy predictors: univariate analysis (Table 10)

No significant gender differences were found in the development of atrophy for any of the measures studied (PBVC, and changes in BPF, WMF and GMF). Age and disease duration were not associated with any of the measures studies (PBVC, and changes in BPF, WMF and GMF). Higher baseline EDSS were predictive of larger PBVC decreases, but no associations were found between EDSS and changes in BPF, WMF and GMF. Baseline MSFC was not associated with any of the measures studies (PBVC, and changes in BPF, WMF and GMF). Significant linear associations were found between Gd-enhancing lesion numbers at baseline and PVBC ($r=-0.458$, $p=0.010$), BPF percentage change ($r=-0.419$, $p=0.019$) and WMF percentage change ($r=-0.532$, $p=0.002$) but not with GMF. BPF percentage change was also associated with baseline proton density lesion load ($r=-0.364$, $p=0.044$).

Table 10. Correlations for PBVC, brain parenchymal fraction, white matter fraction and grey matter fraction percentage changes after 12 months with demographic, clinical and radiological measures at baseline.

		r	p
PBVC	vs age	0.107	0.567
	vs disease duration	0.136	0.466
	vs EDSS*	-0.509	0.003
	vs MSFC	0.190	0.306
	vs proton density lesion load	-0.202	0.275
	vs enhancing lesion number	-0.458	0.010
Brain parenchymal fraction	vs age	0.286	0.119
(% change)	vs disease duration	0.288	0.117
	vs EDSS*	-0.165	0.375
	vs MSFC	0.056	0.763
	vs proton density lesion load	-0.364	0.044
	vs enhancing lesion number	-0.419	0.019
White matter fraction	vs age	0.304	0.096
(% change)	vs disease duration	0.325	0.074
	vs EDSS*	-0.154	0.407
	vs MSFC	0.160	0.390
	vs proton density lesion load	-0.177	0.342
	vs enhancing lesion number	-0.532	0.002
Grey matter fraction	vs age	-0.174	0.349
(% change)	vs disease duration	0.185	0.319
	vs EDSS*	-0.079	0.673
	vs MSFC	-0.012	0.950
	vs proton density lesion load	-0.341	0.060
	vs enhancing lesion number	-0.237	0.199

*All correlation coefficients reported are Pearson correlation coefficients except for EDSS (Spearman); PBVC: percentage brain volume change obtained with SIENAv2.2.

Brain atrophy predictors: stepwise regression models; dependent variables

1) *BPF percentage change over 12 months.* No independent predictor was found in the clinical model; the number of Gd-enhancing lesions was the only independent predictor of brain parenchymal fraction percentage change in both the radiological and combined models (R^2: 0.17; p=0.019).

2) *PBVC over 12 months*. EDSS was found to be an independent predictor when applied to the clinical model (R^2: 0.25; p=0.004); on application of the radiological model the number of enhancing lesions was found to be the only independent predictor (R^2: 0.21; p=0.010). Only EDSS at baseline was found to be independently associated (R^2: 0.25; p=0.004) on the combined model.

3) *WMF percentage change over 12 months.* No independent predictor was found in the clinical model; the number of enhancing lesions was found to be the only independent predictor of white matter fraction percentage change (R^2: 0.28; p=0.002) in the radiological model; on applying the combined model a similar result was obtained, with the number of Gd-enhancing lesions as the only independent predictor (R^2: 0.28; p=0.002).

4) *GMF percentage change over 12 months.* No significant predictors were found in any of the three models.

7. MAGNETIC RESONANCE SPECTROSCOPY FINDINGS

7.1 Baseline

Forty-one patients with early PPMS and 44 control subjects were studied (Table 11). As mentioned in the material and methods section, they were all part of the same cohort investigated in the brain volume studies. Thirty-nine controls and 24 patients yielded usable cortical GM voxels, while 44 controls and 37 patients yielded usable NAWM voxels. No statistically significant differences were found in demographic or clinical variables between patients who provided voxels for cortical GM analyses and those who did not (data not shown).

Table 11. Demographic, clinical and radiological features of patients and controls.

	Controls (n=44)	Patients (n= 41)[1]
Gender (male/female)	50% / 50%	56% / 44%
Age (years)*	36 (23-67)	46 (22-65)
Disease duration (years)**	-	3.31 (2-5)
EDSS*	-	4.5 (3-7)
MSFC**	-	-0.359 (-5.63-1.13)
BPF**	0.83 (0.70-0.87)	0.79 (0.70-0.86)
WMF**	0.28 (0.22-0.32)	0.26 (0.20-0.30)
GMF**	0.55 (0.48-0.59)	0.53 (0.48-0.58)
Number of Gd+ lesions**	-	1.1 (0-9)
Volume of Gd+ lesions (ml)**	-	0.14 (0-0.58)
PD lesion volume (ml)**	-	28.88 (1.43-119.46)

[1]n=40 for brain fractions and Gd values; *median (range); **mean (range); EDSS: Expanded Disability Status Scale; MSFC: Multiple Sclerosis Functional Composite; BPF: Brain parenchymal fraction; WMF: White matter fraction; GMF: Grey matter fraction; Gd+: gadolinium-enhancing; PD: proton density.

Significant differences were seen between patients and controls in metabolite concentrations in cortical GM for tNAA (-12.3% difference in marginal mean values favouring controls; p<0.001) and Glx (-13.9% difference in marginal mean values favouring controls; p=0.005). In NAWM tNAA was reduced (-5.7%; p=0.005) and Ins increased (+14.6%; p=0.002) in patients when compared with controls (Table 12). No differences were observed for any of the other metabolites studied (Cho, Cr and Ins in cortical GM or Cho, Cr and Glx in NAWM).

Table 12. Metabolite concentration in cortical GM & NAWM voxels

	Controls	Patients	p
Cortical GM	n=39	n=24	
Cho[1]	1.105 (0.039)	1.032 (0.052)	0.291
Cr[1]	6.003 (0.126)	5.589 (0.169)	0.067
Ins[1]	4.245 (0.133)	4.504 (0.178)	0.273
tNAA[1]	8.611 (0.144)	7.549 (0.193)	<0.001
Glx[1]	11.485 (0.312)	9.893 (0.417)	0.005
NAWM	n=44	n=37	
Cho[1]	1.262 (0.028)	1.3 (0.031)	0.399
Cr[1]	4.748 (0.072)	4.794 (0.082)	0.693
Ins[1]	3.597 (0.116)	4.211 (0.132)	0.002
tNAA[1]	8.546 (0.104)	8.063 (0.118)	0.005
Glx[1]	7.286 (0.117)	7.152 (0.132)	0.476

GM: grey matter; NAWM: normal appearing white matter; Choline-containing compounds (Cho); Creatine/phosphocreatine (Cr); myo-Inositol (Ins); total N-acetyl-aspartate (tNAA); Glutamate/glutamine (Glx); [1]estimated marginal means (standard error) in mmol/l and p values obtained after linear modeling.

Cortical GM tNAA correlated with EDSS (r=-0.444; p=0.030), MSFC (r=0.487; p=0.016) (Figure 12 A) and with the NHPT (r=0.479; p=0.018). In NAWM, Ins correlated with EDSS (r=0.412; p=0.011) (Figure 12 B), MSFC (r=-0.483; p=0.002), TWT (r=0.371; p=0.024) and NHPT (r=-0.481; p=0.003). Glx levels in NAWM correlated with age (r=-0.328; p=0.048) and with EDSS (r=0.406; p=0.013). In NAWM, Cr correlated with disease duration (r=0.384; p=0.019). No other statistically significant correlations between studied metabolites and clinical or demographical variables were observed.

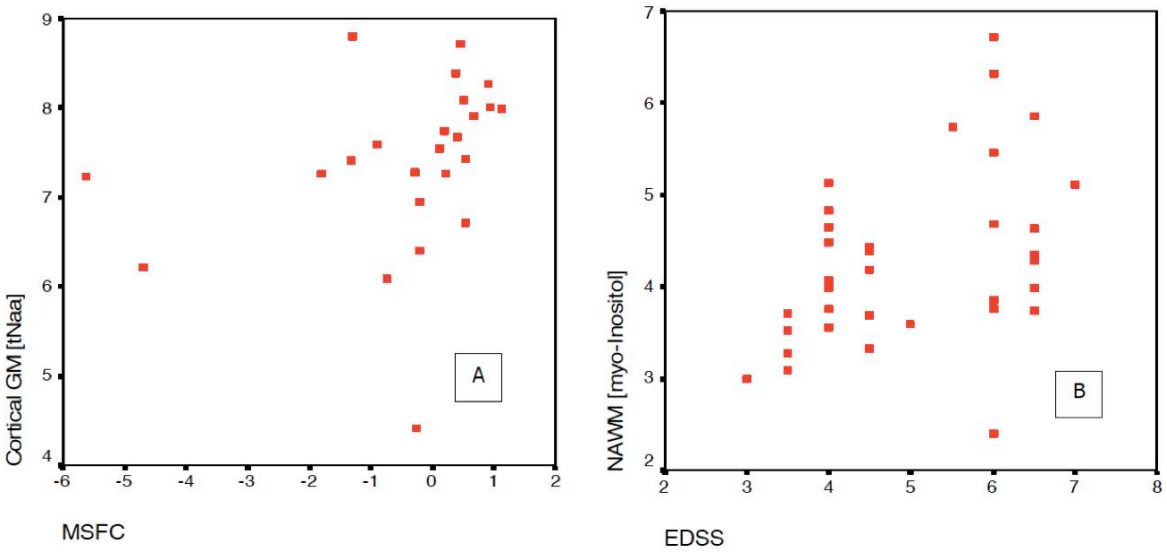

Figure 12. Total N-acetyl-aspartate (tNAA) concentration (mmol/l) in cortical grey matter (GM) [A] and myo-Inositol concentration (mmol/l) in normal appearing white matter (NAWM) [B] voxels of patients plotted against their scores on the Multiple Sclerosis Functional Composite (MSFC) and the Expanded Disability Status Scale (EDSS) respectively.

In cortical GM, tNAA correlated with PD lesion volume (r=-0.449; p=0.028) and with WMF (r=0.554; p=0.006); while Glx correlated with WMF (r=0.473; 0.023). In NAWM, Ins correlated with PD lesion load (r=0.519; p=0.001). No other statistically significant correlations between studied metabolites and radiological variables were observed.

7.2 One year follow-up

The one-year follow-up MRSI sample was made up of 21 early PPMS patients for cortical GM metabolite concentration comparisons, whereas 24 patients made up the sample for NAWM metabolite concentration comparisons. They were all part of the cohort scanned at baseline. Baseline clinical, demographical and radiological features of both subsamples are given in Table 13.

Table 13. Baseline clinical, demographic and radiological features

	Cortical GM (n=21)	NAWM (n= 24)
Sex ratio (male/female)	57% / 43%	62% / 37%
Age at scanning*	45 (26 to 62)	46 (27 to 62)
Disease duration (years)*	3.3 (2 to 5)	3.4 (2 to 5)
EDSS*	4.7 (3.5 to 7)	4.6 (3.5 to 6.5)
MSFC**	-0.18 (1.39)	0.18 (0.63)
Brain parenchymal fraction**	0.796 (0.035)	0.805 (0.030)
White matter fraction**	0.268 (0.018)	0.272 (0.019)
Grey matter fraction**	0.528 (0.026)	0.533 (0.022)
Number of Gd+ lesions**	0.86 (1.52)	0.62 (0.92)
Percentage of patients with Gd+ lesions	42.9 %	41.7 %
PD lesion volume**,***	10.63 (15.26)	6.08 (6.97)

*median (range); **mean (standard deviation); ***lesion volume in ml; NAWM: normal appearing white matter; Gd: gadolinium; EDSS: Expanded Disability Status Scale; MSFC: Multiple Sclerosis Functional Composite; PD: proton density.

The unadjusted comparison between baseline and one-year concentrations of the studied metabolites both in CGM as in NAWM yielded no statistically significant differences (Table 14 for paired t-tests and Wilcoxon signed ranks test).

Table 14. Metabolite concentrations in cortical GM and NAWM voxels at baseline and one-year follow-up timepoints for the studied samples.

	Baseline	One-year follow-up	T-test	Wilcoxon
Cortical GM	n=21	n=21		
Cho[1]	1.21 (0.301)	1.23 (0.272)	0.809	0.821
Cr[1]	5.74 (0.628)	5.72 (0.794)	0.902	0.664
Ins[1]	4.75 (1.013)	4.80 (1.060)	0.796	0.768
tNAA[1]	7.90 (0.712)	8.09 (0.875)	0.415	0.181
Glx[1]	9.90 (1.302)	9.92 (1.547)	0.964	0.958
NAWM	n=24	n=24		
Cho[1]	1.39 (0.167)	1.42 (0.175)	0.397	0.648
Cr[1]	5.24 (0.391)	5.32 (0.639)	0.545	0.475
Ins[1]	4.46 (0.820)	4.65 (1.009)	0.245	0.819
tNAA[1]	8.62 (0.492)	8.58 (0.722)	0.696	0.909
Glx[1]	7.89 (0.672)	8.05 (1.080)	0.547	0.361

GM: grey matter; NAWM: normal appearing white matter; Choline-containing compounds (Cho); Creatine/phosphocreatine (Cr); myo-Inositol (Ins); total N-acetyl-aspartate (tNAA); Glutamate/glutamine (Glx); [1]in mmol/l.

Again, no differences were observed in changes in metabolite concentrations between baseline and one-year follow-up adjusting for the normalized tissue compositions (CSF, GM and WM) of each one of the voxels included in the analysis (at baseline and follow-up). Table 15 displays significance values for each one of the metabolite change variables after adjustment.

Table 15. Adjusted p values for metabolite concentration changes from baseline to one-year timepoints in CGM and NAWM voxels for the studied samples. Columns represent variables adjusted for, indicating the real tissue composition of each one of the voxels included at baseline and at follow-up.

	Baseline			One-year follow-up		
	CSF	White matter	Grey matter	CSF	White matter	Grey matter
Cortical GM						
Cho	0.777	0.795	0.815	0.879	0.813	0.751
Cr	0.850	0.869	0.906	0.869	0.851	0.476
Ins	0.863	0.813	0.802	0.787	0.700	0.683
tNAA	0.906	0.787	0.987	0.580	0.651	0.656
Glx	0.955	0.989	0.952	0.985	0.971	0.959
NAWM						
Cho	0.388	0.537	0.546	0.404	0.402	0.399
Cr	0.400	0.558	0.618	0.552	0.536	0.532
Ins	0.216	0.272	0.291	0.245	0.250	0.246
tNAA	0.629	0.552	0.575	0.701	0.698	0.699
Glx	0.496	0.596	0.617	0.548	0.548	0.548

CSF: cerebrospinal fluid; GM: grey matter; NAWM: normal appearing white matter; Choline-containing compounds (Cho); Creatine/phosphocreatine (Cr); myo-Inositol (Ins); total N-acetyl-aspartate (tNAA); Glutamate/glutamine (Glx).

No attempt was done to search for predictors of brain metabolite changes as no significant changes had been observed for any of the metabolites under scrutiny.

8. DISCUSSION

SUMMARY OF FINDINGS

The results of the present studies can be summarized as follows:

ATROPHY STUDIES

Brain atrophy is present early in the course of PPMS exceeding what is observed in a sample of healthy controls after adjusting for significant variables. Brain atrophy affects GMF and WMF. Both GMF and WMF are related to clinical and MRI lesion-related parameters.

Significant decreases in BPF and GMF can be observed in a period as short as one year, but cannot be detected in the WMF. WMF changes can be predicted by the amount of MRI-visible inflammation at baseline, whereas GMF changes cannot be predicted by any clinical or MRI parameter investigated.

MRSI STUDIES

In cortical GM, concentrations of tNAA and Glx have been found to be lower in patients as compared to control subjects. In NAWM, tNAA has also been found to be reduced (although to a lower extent) and Ins to be increased in patients as compared to control subjects. In cortical GM tNAA levels have been found to be correlated with clinical parameters (tNAA increases meaning better clinical status) and in NAWM Ins has been found to be correlated with clinical parameters (higher levels meaning worse clinical status). Statistically significant correlations between Ins in NAWM and tNAA in cortical GM, in both cases with lesion volume, have also been found to be consistent with opposing effects (higher tNAA levels are associated with lower lesion volumes whereas higher Ins levels are associated with higher lesion volumes).

No changes have been detected in either cortical GM or NAWM for any of the metabolite concentrations after one year of follow-up.

DISCUSSION OF FINDINGS

Results will be initially discussed separately for atrophy and MRSI.

ATROPHY STUDIES

Baseline data

The baseline analysis shows, for the first time, that not only global but also tissue-specific brain atrophy are seen in the early stages of PPMS. Applying full brain tissue segmentation methodologies in PPMS, the baseline analysis demonstrates GM and WM atrophy in early disease. These results extend those of De Stefano et al[120], who found GM atrophy of the neocortex in this group. Comparison with earlier studies is complicated by the use of different methodologies to measure brain atrophy. This is exemplified by studies in relapsing–remitting MS (RRMS)[121-123]. Ge et al[122] found a decrease in WMF (but not in GMF) compared with control subjects. Chard et al[121] found a decrease in both GMF and WMF compared with control subjects, while Quarantelli et al[123] found a decrease in GMF (but not in WMF) compared with control subjects. Hence, different approaches may yield conflicting results, which may also be influenced by differences between the patient cohorts studied. A more recent study[124] including a PPMS cohort (n=50) did not include control subjects, but indicated similar GM volumes (fractions were not calculated) in PPMS as compared to RRMS and patients with clinically isolated syndromes; patients with SPMS had lower values than all other disease subtypes, including PPMS (this has been confirmed by a recent study[125], using voxel-based morphometry). Further studies, using voxel-based morphometry have confirmed the presence of GM atrophy at a regional level[126, 127].

Whole brain and WM atrophy correlate with lesion load in the early stages of PPMS. Significant correlations between atrophy and focal damage and inflammation have been observed in this study for WMF but not for GMF. A previous study in PPMS[38] did not find any cross-sectional relationship between a measure of partial cerebral volume (six central brain slices technique) and brain T2 lesion load. This negative

finding may relate to the fact that the partial cerebral volumes were not normalized to the total intracranial volume. Significant correlations were found between change in lesion load (both T1 and T2) and change in brain volume in the same cohort over 2 years[105]. In RRMS, previous studies performed with similar methodology to that of the present analysis[121-123] found a negative correlation between T2 lesion loads and GMF, but not with WMF. In the present study, T2 lesion load is found to correlate inversely with WMF and this correlation to be non-significant for GMF. Therefore, the results of the present work combined with previous findings would suggest that focal WM damage is related to (i) GM atrophy in RRMS but not in PPMS, and (ii) to WM atrophy in PPMS but not in RRMS. A previous paper studying cortical GM volume loss in RRMS and PPMS supports the first of these findings: a significant correlation between lesion load and cortical atrophy was found in RRMS but not in PPMS subjects[120]. Similarly, Fisher et al[128] reported a significant correlation between MRI parameters and ongoing GM atrophy only in RRMS and not in SPMS. A more recent study by Roosendaal and coworkers[124] seem to challenge this assumption, as lesion volumes seem to correlate with GM volume in a large group of CIS, RRMS, SPMS and PPMS; however, data by disease subtypes are not presented in this latter work.

The absence of an association between focal damage in WM and GM atrophy in PPMS might be taken as an indication that a different process is responsible for GM damage, or that such a process is neurodegenerative in nature and unrelated to focal demyelinating lesions. However, lesions have been long known to occur in GM[129] but have only been recently reappraised thanks to the advent of new MRI techniques which renders a few (but significant) proportion of them visible[130]. Recently, using such methodology, Calabrese et al[131] have shown that cortical lesions are correlated with GM volume and that the presence of cortical lesions is predictive of future development of GM volume loss over follow-up. In PPMS, such a close relationship between GM atrophy development and cortical lesions may obscure a possible relation between white matter lesions and GM atrophy. Finally, the presence of a further parallel neurodegenerative process mostly affecting GM tissue cannot be ruled out.

The present study shows that whole brain and GM and WM atrophy are related to the development of disability in patients with early PPMS. Previous studies in patients with PPMS have either failed to show any correlation between atrophy and disability or, if found, they have been very weak. In one study[132], no correlations were found, with either EDSS or MSFC, in 20 patients with PPMS using a normalized measure of whole brain atrophy. In another study[133], no correlation between EDSS and ventricular volumes was found in a group of 31 patients, but a significant correlation was found between the pyramidal functional system and ventricular volume. Stevenson et al.[38], studying 158 patients with PPMS, found a weak but significant correlation between a brain partial volume measure and EDSS. One probable explanation for the strong correlations found in the present work may relate to the fact that the population studied was in the early clinical stage of the condition. The cohort studied has a wide range of EDSS values (from 3 to 7 with a median of 4.5), and perhaps more importantly their disability is, by definition, recently acquired. Another explanation perhaps lies in the methodology used, a normalized method, which reduces the effect of inter-individual variations for head size and is much more powerful in cross-sectional studies than non-normalized measures[134]. Posteriorly, many studies both in PPMS[107, 120, 135] and in other disease phenotypes[107, 124, 128, 136] have definitely established the existence of a significant association between whole brain and WM and GM atrophy and disability. The results of the present study in which GMF correlates significantly with the NHPT and with borderline significance with the PASAT but does not correlate with other measures more heavily weighted towards locomotion, such as the TWT or EDSS, are as it might be anticipated on clinical grounds. This is somewhat at odds with recent studies in other disease phenotypes where correlations between GM and disability were found to be stronger than for white matter[128, 136]. Most likely, a differential impact of grey and white matter atrophy on disability aspects is to be expected, as shown for cognitive impairment[137]. In this regard, it has also been recently shown in PPMS that regionally specific GM atrophy correlates with cognitive impairment[138].

One-year follow-up data

Changes in grey but not white matter volume can be detected in patients with clinically early PPMS over 1 year. Changes in atrophy have been detected in patients with established PPMS over 1 year using non-normalized partial brain measures[104]. This has also been shown, using longer follow-up times, for normalized global brain measures[139]. The present study suggests that, over the short term, the development of atrophy in patients with early PPMS is due mainly to change in GM. It is also worth noting that the observed decrease in GMF seems to be a real finding and not a methodological artefact, as it occurs in spite of the bias in SPM segmentation, whereby in subjects with increasing lesion loads SPM tends to overestimate GM volumes[60]. Later work has shown GM atrophy to preferentially take place at specific cortical and subcortical regions[127]. A possible explanation for these findings would be that inflammation and gliosis may be obscuring white matter volume loss, whereas GM tissue loss occurs without reactive gliosis or inflammation that may mask volume loss[140]. The present findings are also consistent with two longitudinal studies which have assessed the evolution of grey and white matter atrophy in patients with clinically isolated syndromes[141] and relapsing–remitting multiple sclerosis[142] which have used the same methodology. Both studies found a significant decrease in GMF with no concomitant decrease in WMF.

The number of Gd-enhancing lesions predicts the development of WM atrophy but not of GM volume loss. Many studies have assessed the effect of enhancing lesions on subsequent brain volume changes in relapsing–remitting multiple sclerosis[57, 143-145] clinically isolated syndromes suggestive of multiple sclerosis[141, 146] and secondary progressive multiple sclerosis[147]. Most have found that large volumes of enhancing lesions are predictive of or associated with the development of atrophy. We are not aware of any similar studies in patients with PPMS. Resolution of inflammation-associated oedema is likely to be an important contributing factor in WM volume changes, but the contribution of inflammation to subsequent WM tissue loss cannot be ruled out. Ensuing gliosis, which might prevent volume loss, might complicate the picture even further. In this regard, Inglese and colleagues have shown, in a group

of patients with rapidly evolving secondary progressive multiple sclerosis and a percentage of annual global tissue loss of -1.88%, that even after suppression of inflammation through therapy with autologous haematopoietic stem cell transplantation, subsequent brain atrophy development is still marginally associated with the enhancing lesion load prior to treatment[147]. Interestingly, our failure to predict GM atrophy from the baseline number of gadolinium-enhancing lesions might indicate that GM tissue damage is not related (or at least not mostly) to white matter lesions (as already indicated by the lack of correlation between white matter MRI lesional parameters found in the baseline analysis of this cohort) and that the pseudoatrophy effects occurring in white matter are not visible in the GM compartment, probably reflecting the lower inflammatory nature of cortical[140] and deep[148] GM lesions. The independence of GM tissue loss from gross inflammation may make the measurement of GM volume changes a useful surrogate for the assessment of new neuroprotective strategies in multiple sclerosis.

Role of methodology. The estimated percentage global tissue loss in this study for SPM-based methodology (-1.03%) and for SIENAv2.2 (-0.63%) are within the range seen in different phenotypes of multiple sclerosis, which goes from -0.46[141] to -1.9%[149], calculated with a range of different atrophy techniques. Although separate grey and white matter volumes cannot be obtained, SIENA is more user-friendly as it needs no manual operator input and the software is freely available on the World-Wide Web in a compact package. Conversely, SPM-derived methods need considerable operator input (lesion contouring) and, even though it can also be downloaded from the World-Wide Web, licensed software is required[50]. Estimates of atrophy are known to differ depending on the segmentation procedure and pulse sequence used for their estimation[150, 151]. SPM segmentation is biased by the presence of lesions, although this bias seems to have an effect on grey and white matter only and not whole-brain estimates[60]. A trend for underestimation of higher atrophy has been reported with SIENA[61]. More methodological studies are warranted before the present findings can be fully explained.

MRSI STUDIES

Baseline data

Studies of patients affected by PPMS with established disease have shown decreased tNAA/creatine-phosphocreatine or tNAA concentrations in NAWM[152-154]. The present study extends these findings to the early clinical stages of PPMS, and, to our knowledge, was the first study to report on abnormalities of cortical GM metabolites in PPMS. Although the magnitude of the tNAA level decrease appeared greater in cortical GM than in NAWM (mean decrease −12.3% vs −5.7%), the number of voxel and subjects available for cortical GM analysis was fewer and the potential for partial volume effects to influence cortical GM findings was greater. Nevertheless, since robust methods were used to address partial volume effects, the observed decrease in cortical GM tNAA concentration is likely to be a real biological finding, suggesting that neuronal dysfunction or loss occurs in the early stages of PPMS. Although high levels of NAWM Ins have been recently found in patients with RRMS[118] and clinically isolated syndromes[155] to our knowledge, our study was the first to demonstrate an increase in the levels of NAWM Ins in patients with PPMS. Previous studies with MRS have identified Ins as a potential marker of astroglia[77], and histopathological studies in MS suggest that astrogliosis is a prominent abnormality in NAWM[156]. Decreased glutamate-glutamine concentrations have not been reported previously in cortical GM of patients with PPMS. Although these two metabolites are closely associated in the brain[157], the concentration of glutamate is higher in neurons[158, 159] while that of glutamine is higher in glial cells[158]. Therefore, although the present results appear consistent with cortical GM neuronal metabolic impairment or loss, further studies using techniques to resolve glutamate-glutamine signals are needed to clarify this issue.

In this study we found a moderate correlation between tNAA levels in cortical GM and disability, suggesting that cortical GM neuronal dysfunction or loss has an influence on clinical status in PPMS. A relationship was not found between tNAA levels in NAWM and disability, consistent with most previous PPMS study findings

(being found in only 1[153] of 3 studies[152, 153, 160]) but differing from studies in RRMS[161, 162]. The correlation of NAWM Ins concentration with disability is remarkably concordant with studies of patients with RRMS[118] and would suggest that Ins is a marker of clinical progression in MS, although the mechanism is unclear. Measurements of Ins concentration in NAWM may be of value in monitoring the effect of potential therapeutic agents. A positive correlation between NAWM glutamate-glutamine concentration and the EDSS score has been found, suggesting that increasing concentrations of glutamate, glutamine, or both relate to worsening clinical status in patients with early PPMS. The present method cannot confirm whether this correlation relates to increased glial cellullarity (increased glutamine concentration), increased excitotoxic reaction (increased extracellular glutamate concentration), or both.

Magnetic resonance lesion volume and atrophy in WM correlated with tNAA concentration in CGM, but not in NAWM, suggesting that WM disease influences the function or integrity of cortical neurons. The correlation between lesion volume and Ins concentration in NAWM has also been shown in RRMS[118].

One-year follow-up data

Changes for any of the metabolites studied were not detected either in the CGM or in the NAWM both in adjusted and unadjusted models. These results are in keeping with those of an early cohort of RRMS followed for two years using the same methodology, as no changes for any of the metabolites were also observed[163]. Similarly, a four centre 3-year follow-up study[164] of 58 patients with PPMS embedded in the PROMISE[40] trial (n=943) did not detect any significant temporal changes in metabolite ratios in the two groups of patients (treated and not treated with glatiramer acetate) relative to baseline values during the study period.

It is probable that the reported suboptimal reproducibility of MRS techniques is partly responsible for the lack of significant changes over follow-up in our work and in the

abovementioned studies by Tibero et al[163] and Sajja et al[164]. In comparison to the brain volume methodology utilized in the studies which are part of this thesis, with a reproducibility in the range of 1% (coefficient of variation)[60], the MRSI studies were obtained with a processing pipeline with a reported reproducibility of around 10% (depending on the specific metabolite)[165], which is comparable to reproducibility reported by other groups[101, 166, 167]. It is therefore not surprising that small changes over one year might not be detected using MRSI. This may be compounded by the fact that, in order to obtain cortical GM and NAWM voxels that are not containing lesions or other types of tissue, our strict inclusion criteria produced a sample size significantly smaller in the follow-up analysis as compared to the baseline cross-sectional study. Whereas in the baseline analysis 1115 voxels were usable for the NAWM comparison (724 from controls and 391 from patients) and 154 voxels for the cortical GM comparison (113 from controls and 41 from patients), in the follow-up analysis numbers of available voxels went down to 587 voxels for NAWM (322 from baseline and 265 from follow-up) and to 128 voxels for cortical GM (70 from baseline and 58 from follow-up). Finally, metabolite changes may be partially reversible, as is the case of tNAA, reflecting functional and/or sub-lethal neuronal damage[168].

10. CONCLUSIONS

In patients with PPMS early in their clinical course:

1. Disease-related brain volume loss is already present and affects both grey and white matter tissue fractions.

2. Significant grey matter volume loss occurs over a period of one year and cannot be predicted using clinical and MRI lesion-related parameters.

3. Significant white matter changes are not seen at a group level over one year, but can be predicted by the presence of gadolinium-enhancing lesions at baseline, indicating, at least partially, the existence of a pseudoatrophy effect.

Overall, this would point to grey matter volume measurement as an interesting surrogate in treatment trials for neuroprotective strategies, as it does not seem to be affected by the termination of MRI visible white matter inflammation.

4. Significant differences have been observed in the concentration of brain metabolites (namely tNAA decreases in cortical grey matter and Ins increases in normal appearing white matter) between patients and controls.

5. Significant correlations have been observed between clinical and MRI parameters and metabolite concentrations

6. No longitudinal changes over one year have been detected in the concentration of any of the metabolites studied

11. REFERENCES

1. Noseworthy JH, Lucchinetti C, Rodriguez M, Weinshenker BG. Multiple sclerosis. The New England journal of medicine 2000;343:938-952.

2. Compston A, Coles A. Multiple sclerosis. Lancet 2008;372:1502-1517.

3. Trapp BD, Peterson J, Ransohoff RM, Rudick R, Mork S, Bo L. Axonal transection in the lesions of multiple sclerosis. The New England journal of medicine 1998;338:278-285.

4. Murray TJ. The history of multiple sclerosis: the changing frame of the disease over the centuries. Journal of the neurological sciences 2009;277 Suppl 1:S3-8.

5. R C. Pathological anatomy: illustrations of the elementary forms of disease. London: Longman, Orme, Brown, Green and Longman, 1838.

6. Lublin FD, Reingold SC. Defining the clinical course of multiple sclerosis: results of an international survey. National Multiple Sclerosis Society (USA) Advisory Committee on Clinical Trials of New Agents in Multiple Sclerosis. Neurology 1996;46:907-911.

7. Lublin FD, Reingold SC, Cohen JA, et al. Defining the clinical course of multiple sclerosis: the 2013 revisions. Neurology 2014;83:278-286.

8. Kremenchutzky M, Cottrell D, Rice G, et al. The natural history of multiple sclerosis: a geographically based study. 7. Progressive-relapsing and relapsing-progressive multiple sclerosis: a re-evaluation. Brain : a journal of neurology 1999;122 (Pt 10):1941-1950.

9. Tremlett H, Paty D, Devonshire V. The natural history of primary progressive MS in British Columbia, Canada. Neurology 2005;65:1919-1923.

10. Tintore M, Rovira A, Rio J, et al. Baseline MRI predicts future attacks and disability in clinically isolated syndromes. Neurology 2006;67:968-972.

11. Koch-Henriksen N, Sorensen PS. The changing demographic pattern of multiple sclerosis epidemiology. Lancet neurology 2010;9:520-532.

12. Thompson AJ, Polman CH, Miller DH, et al. Primary progressive multiple sclerosis. Brain : a journal of neurology 1997;120 (Pt 6):1085-1096.

13. Hafler DA, Compston A, Sawcer S, et al. Risk alleles for multiple sclerosis identified by a genomewide study. The New England journal of medicine 2007;357:851-862.

14. Fenoglio C, Scalabrini D, Esposito F, et al. Progranulin gene variability increases the risk for primary progressive multiple sclerosis in males. Genes and immunity 2010;11:497-503.

15. Camina-Tato M, Fernandez M, Morcillo-Suarez C, et al. Genetic association of CASP8 polymorphisms with primary progressive multiple sclerosis. Journal of neuroimmunology 2010;222:70-75.

16. de Jong BA, Westendorp RG, Eskdale J, Uitdehaag BM, Huizinga TW. Frequency of functional interleukin-10 promoter polymorphism is different between relapse-onset and primary progressive multiple sclerosis. Human immunology 2002;63:281-285.

17. Vasconcelos CC, Fernandez O, Leyva L, Thuler LC, Alvarenga RM. Does the DRB1*1501 allele confer more severe and faster progression in primary progressive multiple sclerosis patients? HLA in primary progressive multiple sclerosis. Journal of neuroimmunology 2009;214:101-103.

18. Cree BA. Genetics of primary progressive multiple sclerosis. Handbook of clinical neurology 2014;122:211-230.

19. Miller DH, Leary SM. Primary-progressive multiple sclerosis. Lancet neurology 2007;6:903-912.

20. Cottrell DA, Kremenchutzky M, Rice GP, et al. The natural history of multiple sclerosis: a geographically based study. 5. The clinical features and natural history of primary progressive multiple sclerosis. Brain : a journal of neurology 1999;122 (Pt 4):625-639.

21. Confavreux C, Vukusic S. Natural history of multiple sclerosis: a unifying concept. Brain : a journal of neurology 2006;129:606-616.

22. Kremenchutzky M, Rice GP, Baskerville J, Wingerchuk DM, Ebers GC. The natural history of multiple sclerosis: a geographically based study 9: observations on the progressive phase of the disease. Brain : a journal of neurology 2006;129:584-594.

23. Scalfari A, Neuhaus A, Daumer M, Ebers GC, Muraro PA. Age and disability accumulation in multiple sclerosis. Neurology 2011;77:1246-1252.

24. Bruck W, Lucchinetti C, Lassmann H. The pathology of primary progressive multiple sclerosis. Mult Scler 2002;8:93-97.

25. Magliozzi R, Howell O, Vora A, et al. Meningeal B-cell follicles in secondary progressive multiple sclerosis associate with early onset of disease and severe cortical pathology. Brain : a journal of neurology 2007;130:1089-1104.

26. Kutzelnigg A, Lucchinetti CF, Stadelmann C, et al. Cortical demyelination and diffuse white matter injury in multiple sclerosis. Brain : a journal of neurology 2005;128:2705-2712.

27. Antel J, Antel S, Caramanos Z, Arnold DL, Kuhlmann T. Primary progressive multiple sclerosis: part of the MS disease spectrum or separate disease entity? Acta neuropathologica 2012.

28. Miller DH, Weinshenker BG, Filippi M, et al. Differential diagnosis of suspected multiple sclerosis: a consensus approach. Mult Scler 2008;14:1157-1174.

29. Charil A, Yousry TA, Rovaris M, et al. MRI and the diagnosis of multiple sclerosis: expanding the concept of "no better explanation". Lancet neurology 2006;5:841-852.

30. Poser CM, Paty DW, Scheinberg L, et al. New diagnostic criteria for multiple sclerosis: guidelines for research protocols. Annals of neurology 1983;13:227-231.

31. Thompson AJ, Montalban X, Barkhof F, et al. Diagnostic criteria for primary progressive multiple sclerosis: a position paper. Annals of neurology 2000;47:831-835.

32. McDonald WI, Compston A, Edan G, et al. Recommended diagnostic criteria for multiple sclerosis: guidelines from the International Panel on the diagnosis of multiple sclerosis. Annals of neurology 2001;50:121-127.

33. Polman CH, Reingold SC, Edan G, et al. Diagnostic criteria for multiple sclerosis: 2005 revisions to the "McDonald Criteria". Annals of neurology 2005;58:840-846.

34. Polman CH, Reingold SC, Banwell B, et al. Diagnostic criteria for multiple sclerosis: 2010 revisions to the McDonald criteria. Annals of neurology 2011;69:292-302.

35. Montalban X, Sastre-Garriga J, Filippi M, et al. Primary progressive multiple sclerosis diagnostic criteria: a reappraisal. Mult Scler 2009;15:1459-1465.

36. Leary SM, Miller DH, Stevenson VL, Brex PA, Chard DT, Thompson AJ. Interferon beta-1a in primary progressive MS: an exploratory, randomized, controlled trial. Neurology 2003;60:44-51.

37. Montalban X, Sastre-Garriga J, Tintore M, et al. A single-center, randomized, double-blind, placebo-controlled study of interferon beta-1b on primary progressive and transitional multiple sclerosis. Mult Scler 2009;15:1195-1205.

38. Stevenson VL, Miller DH, Rovaris M, et al. Primary and transitional progressive MS: a clinical and MRI cross-sectional study. Neurology 1999;52:839-845.

39. Tur C, Montalban X, Tintore M, et al. Interferon beta-1b for the treatment of primary progressive multiple sclerosis: five-year clinical trial follow-up. Archives of neurology 2011;68:1421-1427.

40. Wolinsky JS, Narayana PA, O'Connor P, et al. Glatiramer acetate in primary progressive multiple sclerosis: results of a multinational, multicenter, double-blind, placebo-controlled trial. Annals of neurology 2007;61:14-24.

41. Kalkers NF, Barkhof F, Bergers E, van Schijndel R, Polman CH. The effect of the neuroprotective agent riluzole on MRI parameters in primary progressive multiple sclerosis: a pilot study. Mult Scler 2002;8:532-533.

42. Hawker K, O'Connor P, Freedman MS, et al. Rituximab in patients with primary progressive multiple sclerosis: results of a randomized double-blind placebo-controlled multicenter trial. Annals of neurology 2009;66:460-471.

43. Cohen JA, Barkhof F, Comi G, et al. Oral fingolimod or intramuscular interferon for relapsing multiple sclerosis. The New England journal of medicine 2010;362:402-415.

44. Kappos L, Radue EW, O'Connor P, et al. A placebo-controlled trial of oral fingolimod in relapsing multiple sclerosis. The New England journal of medicine 2010;362:387-401.

45. Calabresi PA, Radue EW, Goodin D, et al. Safety and efficacy of fingolimod in patients with relapsing-remitting multiple sclerosis (FREEDOMS II): a double-blind, randomised, placebo-controlled, phase 3 trial. Lancet neurology 2014;13:545-556.

46. Romme Christensen J, Ratzer R, Bornsen L, et al. Natalizumab in progressive MS: Results of an open-label, phase 2A, proof-of-concept trial. Neurology 2014;82:1499-1507.

47. Comi G, Jeffery D, Kappos L, et al. Placebo-controlled trial of oral laquinimod for multiple sclerosis. The New England journal of medicine 2012;366:1000-1009.

48. Vollmer TL, Sorensen PS, Selmaj K, et al. A randomized placebo-controlled phase III trial of oral laquinimod for multiple sclerosis. Journal of neurology 2014;261:773-783.

49. Khan O, Miller AE, Tornatore C, Phillips JT, Barnes CJ. Practice patterns of US neurologists in patients with SPMS and PPMS: A consensus study. Neurology Clinical practice 2012;2:58-66.

50. Vrenken H, Jenkinson M, Horsfield MA, et al. Recommendations to improve imaging and analysis of brain lesion load and atrophy in longitudinal studies of multiple sclerosis. Journal of neurology 2013;260:2458-2471.

51. Bakshi R, Benedict RH, Bermel RA, Jacobs L. Regional brain atrophy is associated with physical disability in multiple sclerosis: semiquantitative magnetic resonance imaging and relationship to clinical findings. Journal of neuroimaging : official journal of the American Society of Neuroimaging 2001;11:129-136.

52. Simon JH, Jacobs LD, Campion MK, et al. A longitudinal study of brain atrophy in relapsing multiple sclerosis. The Multiple Sclerosis Collaborative Research Group (MSCRG). Neurology 1999;53:139-148.

53. Rovaris M, Inglese M, van Schijndel RA, et al. Sensitivity and reproducibility of volume change measurements of different brain portions on magnetic resonance imaging in patients with multiple sclerosis. Journal of neurology 2000;247:960-965.

54. Sailer M, Fischl B, Salat D, et al. Focal thinning of the cerebral cortex in multiple sclerosis. Brain : a journal of neurology 2003;126:1734-1744.

55. Bermel RA, Bakshi R. The measurement and clinical relevance of brain atrophy in multiple sclerosis. Lancet neurology 2006;5:158-170.

56. Anderson VM, Fox NC, Miller DH. Magnetic resonance imaging measures of brain atrophy in multiple sclerosis. Journal of magnetic resonance imaging : JMRI 2006;23:605-618.

57. Rudick RA, Fisher E, Lee JC, Simon J, Jacobs L. Use of the brain parenchymal fraction to measure whole brain atrophy in relapsing-remitting MS. Multiple Sclerosis Collaborative Research Group. Neurology 1999;53:1698-1704.

58. Brass SD, Narayanan S, Antel JP, Lapierre Y, Collins L, Arnold DL. Axonal damage in multiple sclerosis patients with high versus low expanded disability status scale score. The Canadian journal of neurological sciences Le journal canadien des sciences neurologiques 2004;31:225-228.

59. Ashburner J, Friston K. Multimodal image coregistration and partitioning--a unified framework. NeuroImage 1997;6:209-217.

60. Chard DT, Parker GJ, Griffin CM, Thompson AJ, Miller DH. The reproducibility and sensitivity of brain tissue volume measurements derived from an SPM-based segmentation methodology. Journal of magnetic resonance imaging : JMRI 2002;15:259-267.

61. Smith SM, Zhang Y, Jenkinson M, et al. Accurate, robust, and automated longitudinal and cross-sectional brain change analysis. NeuroImage 2002;17:479-489.

62. Ge Y, Grossman RI, Udupa JK, et al. Brain atrophy in relapsing-remitting multiple sclerosis and secondary progressive multiple sclerosis: longitudinal quantitative analysis. Radiology 2000;214:665-670.

63. Kovacevic N, Lobaugh NJ, Bronskill MJ, Levine B, Feinstein A, Black SE. A robust method for extraction and automatic segmentation of brain images. NeuroImage 2002;17:1087-1100.

64. Freeborough PA, Fox NC, Kitney RI. Interactive algorithms for the segmentation and quantitation of 3-D MRI brain scans. Computer methods and programs in biomedicine 1997;53:15-25.

65. Fox NC, Freeborough PA. Brain atrophy progression measured from registered serial MRI: validation and application to Alzheimer's disease. Journal of magnetic resonance imaging : JMRI 1997;7:1069-1075.

66. Smith SM, De Stefano N, Jenkinson M, Matthews PM. Normalized accurate measurement of longitudinal brain change. Journal of computer assisted tomography 2001;25:466-475.

67. Fox NC, Jenkins R, Leary SM, et al. Progressive cerebral atrophy in MS: a serial study using registered, volumetric MRI. Neurology 2000;54:807-812.

68. Smith SM. Fast robust automated brain extraction. Human brain mapping 2002;17:143-155.

69. Jenkinson M, Smith S. A global optimisation method for robust affine registration of brain images. Medical image analysis 2001;5:143-156.

70. Jenkinson M, Bannister P, Brady M, Smith S. Improved optimization for the robust and accurate linear registration and motion correction of brain images. NeuroImage 2002;17:825-841.

71. Zhang Y, Brady M, Smith S. Segmentation of brain MR images through a hidden Markov random field model and the expectation-maximization algorithm. IEEE transactions on medical imaging 2001;20:45-57.

72. Sajja BR, Wolinsky JS, Narayana PA. Proton magnetic resonance spectroscopy in multiple sclerosis. Neuroimaging clinics of North America 2009;19:45-58.

73. De Stefano N, Filippi M, Miller D, et al. Guidelines for using proton MR spectroscopy in multicenter clinical MS studies. Neurology 2007;69:1942-1952.

74. Simmons ML, Frondoza CG, Coyle JT. Immunocytochemical localization of N-acetyl-aspartate with monoclonal antibodies. Neuroscience 1991;45:37-45.

75. Patel TB, Clark JB. Synthesis of N-acetyl-L-aspartate by rat brain mitochondria and its involvement in mitochondrial/cytosolic carbon transport. The Biochemical journal 1979;184:539-546.

76. Daikhin Y, Yudkoff M. Compartmentation of brain glutamate metabolism in neurons and glia. The Journal of nutrition 2000;130:1026S-1031S.

77. Brand A, Richter-Landsberg C, Leibfritz D. Multinuclear NMR studies on the energy metabolism of glial and neuronal cells. Developmental neuroscience 1993;15:289-298.

78. Bitsch A, Bruhn H, Vougioukas V, et al. Inflammatory CNS demyelination: histopathologic correlation with in vivo quantitative proton MR spectroscopy. AJNR American journal of neuroradiology 1999;20:1619-1627.

79. Brockmann K, Dechent P, Wilken B, Rusch O, Frahm J, Hanefeld F. Proton MRS profile of cerebral metabolic abnormalities in Krabbe disease. Neurology 2003;60:819-825.

80. Wyss M, Kaddurah-Daouk R. Creatine and creatinine metabolism. Physiological reviews 2000;80:1107-1213.

81. Rigotti DJ, Inglese M, Gonen O. Whole-brain N-acetylaspartate as a surrogate marker of neuronal damage in diffuse neurologic disorders. AJNR American journal of neuroradiology 2007;28:1843-1849.

82. Rigotti DJ, Inglese M, Babb JS, et al. Serial whole-brain N-acetylaspartate concentration in healthy young adults. AJNR American journal of neuroradiology 2007;28:1650-1651.

83. Gonen O, Catalaa I, Babb JS, et al. Total brain N-acetylaspartate: a new measure of disease load in MS. Neurology 2000;54:15-19.

84. Bertholdo D, Watcharakorn A, Castillo M. Brain proton magnetic resonance spectroscopy: introduction and overview. Neuroimaging clinics of North America 2013;23:359-380.

85. Li BS, Wang H, Gonen O. Metabolite ratios to assumed stable creatine level may confound the quantification of proton brain MR spectroscopy. Magnetic resonance imaging 2003;21:923-928.

86. Jansen JF, Backes WH, Nicolay K, Kooi ME. 1H MR spectroscopy of the brain: absolute quantification of metabolites. Radiology 2006;240:318-332.

87. Provencher SW. Automatic quantitation of localized in vivo 1H spectra with LCModel. NMR in biomedicine 2001;14:260-264.

88. Raz N, Rodrigue KM. Differential aging of the brain: patterns, cognitive correlates and modifiers. Neuroscience and biobehavioral reviews 2006;30:730-748.

89. Scahill RI, Frost C, Jenkins R, Whitwell JL, Rossor MN, Fox NC. A longitudinal study of brain volume changes in normal aging using serial registered magnetic resonance imaging. Archives of neurology 2003;60:989-994.

90. Ge Y, Grossman RI, Babb JS, Rabin ML, Mannon LJ, Kolson DL. Age-related total gray matter and white matter changes in normal adult brain. Part I: volumetric MR imaging analysis. AJNR American journal of neuroradiology 2002;23:1327-1333.

91. Raz N, Lindenberger U, Rodrigue KM, et al. Regional brain changes in aging healthy adults: general trends, individual differences and modifiers. Cereb Cortex 2005;15:1676-1689.

92. Giedd JN, Blumenthal J, Jeffries NO, et al. Brain development during childhood and adolescence: a longitudinal MRI study. Nature neuroscience 1999;2:861-863.

93. Brooks JC, Roberts N, Kemp GJ, Gosney MA, Lye M, Whitehouse GH. A proton magnetic resonance spectroscopy study of age-related changes in frontal lobe metabolite concentrations. Cereb Cortex 2001;11:598-605.

94. Christiansen P, Toft P, Larsson HB, Stubgaard M, Henriksen O. The concentration of N-acetyl aspartate, creatine + phosphocreatine, and choline in different parts of the brain in adulthood and senium. Magnetic resonance imaging 1993;11:799-806.

95. Driscoll I, Hamilton DA, Petropoulos H, et al. The aging hippocampus: cognitive, biochemical and structural findings. Cereb Cortex 2003;13:1344-1351.

96. Moreno-Torres A, Pujol J, Soriano-Mas C, Deus J, Iranzo A, Santamaria J. Age-related metabolic changes in the upper brainstem tegmentum by MR spectroscopy. Neurobiology of aging 2005;26:1051-1059.

97. Leary SM, Brex PA, MacManus DG, et al. A (1)H magnetic resonance spectroscopy study of aging in parietal white matter: implications for trials in multiple sclerosis. Magnetic resonance imaging 2000;18:455-459.

98. Pfefferbaum A, Adalsteinsson E, Spielman D, Sullivan EV, Lim KO. In vivo spectroscopic quantification of the N-acetyl moiety, creatine, and choline from large volumes of brain gray and white matter: effects of normal aging. Magnetic resonance

in medicine : official journal of the Society of Magnetic Resonance in Medicine / Society of Magnetic Resonance in Medicine 1999;41:276-284.

99. Sijens PE, den Heijer T, Origgi D, et al. Brain changes with aging: MR spectroscopy at supraventricular plane shows differences between women and men. Radiology 2003;226:889-896.

100. Adalsteinsson E, Sullivan EV, Kleinhans N, Spielman DM, Pfefferbaum A. Longitudinal decline of the neuronal marker N-acetyl aspartate in Alzheimer's disease. Lancet 2000;355:1696-1697.

101. Kirov, II, George IC, Jayawickrama N, Babb JS, Perry NN, Gonen O. Longitudinal inter- and intra-individual human brain metabolic quantification over 3 years with proton MR spectroscopy at 3 T. Magnetic resonance in medicine : official journal of the Society of Magnetic Resonance in Medicine / Society of Magnetic Resonance in Medicine 2012;67:27-33.

102. Thompson AJ, Kermode AG, MacManus DG, et al. Patterns of disease activity in multiple sclerosis: clinical and magnetic resonance imaging study. BMJ 1990;300:631-634.

103. Thompson AJ, Kermode AG, Wicks D, et al. Major differences in the dynamics of primary and secondary progressive multiple sclerosis. Annals of neurology 1991;29:53-62.

104. Stevenson VL, Miller DH, Leary SM, et al. One year follow up study of primary and transitional progressive multiple sclerosis. Journal of neurology, neurosurgery, and psychiatry 2000;68:713-718.

105. Ingle GT, Stevenson VL, Miller DH, et al. Two-year follow-up study of primary and transitional progressive multiple sclerosis. Mult Scler 2002;8:108-114.

106. Sastre-Garriga J, Ingle GT, Rovaris M, et al. Long-term clinical outcome of primary progressive MS: predictive value of clinical and MRI data. Neurology 2005;65:633-635.

107. Khaleeli Z, Ciccarelli O, Manfredonia F, et al. Predicting progression in primary progressive multiple sclerosis: a 10-year multicenter study. Annals of neurology 2008;63:790-793.

108. Ingle GT, Sastre-Garriga J, Miller DH, Thompson AJ. Is inflammation important in early PPMS? a longitudinal MRI study. Journal of neurology, neurosurgery, and psychiatry 2005;76:1255-1258.

109. Bieniek M, Altmann DR, Davies GR, et al. Cord atrophy separates early primary progressive and relapsing remitting multiple sclerosis. Journal of neurology, neurosurgery, and psychiatry 2006;77:1036-1039.

110. Bodini B, Battaglini M, De Stefano N, et al. T2 lesion location really matters: a 10 year follow-up study in primary progressive multiple sclerosis. Journal of neurology, neurosurgery, and psychiatry 2011;82:72-77.

111. Sastre-Garriga J, Tintore M. Multiple sclerosis: Lesion location may predict disability in multiple sclerosis. Nature reviews Neurology 2010;6:648-649.

112. Rocca MA, Absinta M, Filippi M. The role of advanced magnetic resonance imaging techniques in primary progressive MS. Journal of neurology 2012;259:611-621.

113. Kurtzke JF. Rating neurologic impairment in multiple sclerosis: an expanded disability status scale (EDSS). Neurology 1983;33:1444-1452.

114. Cutter GR, Baier ML, Rudick RA, et al. Development of a multiple sclerosis functional composite as a clinical trial outcome measure. Brain : a journal of neurology 1999;122 (Pt 5):871-882.

115. Fischer JS, Rudick RA, Cutter GR, Reingold SC. The Multiple Sclerosis Functional Composite Measure (MSFC): an integrated approach to MS clinical outcome assessment. National MS Society Clinical Outcomes Assessment Task Force. Mult Scler 1999;5:244-250.

116. Fischer J, Jak A, Kniker J, Rudick R, Cutter G. Administration and scoring manual for the MS Functional Composite measure (MSFC). New York: Demos, 1999.

117. McLean MA, Woermann FG, Barker GJ, Duncan JS. Quantitative analysis of short echo time (1)H-MRSI of cerebral gray and white matter. Magnetic resonance in medicine : official journal of the Society of Magnetic Resonance in Medicine / Society of Magnetic Resonance in Medicine 2000;44:401-411.

118. Chard DT, Griffin CM, McLean MA, et al. Brain metabolite changes in cortical grey and normal-appearing white matter in clinically early relapsing-remitting multiple sclerosis. Brain : a journal of neurology 2002;125:2342-2352.

119. Perneger TV. What's wrong with Bonferroni adjustments. BMJ 1998;316:1236-1238.

120. De Stefano N, Matthews PM, Filippi M, et al. Evidence of early cortical atrophy in MS: relevance to white matter changes and disability. Neurology 2003;60:1157-1162.

121. Chard DT, Griffin CM, Parker GJ, Kapoor R, Thompson AJ, Miller DH. Brain atrophy in clinically early relapsing-remitting multiple sclerosis. Brain : a journal of neurology 2002;125:327-337.

122. Ge Y, Grossman RI, Udupa JK, Babb JS, Nyul LG, Kolson DL. Brain atrophy in relapsing-remitting multiple sclerosis: fractional volumetric analysis of gray matter and white matter. Radiology 2001;220:606-610.

123. Quarantelli M, Ciarmiello A, Morra VB, et al. Brain tissue volume changes in relapsing-remitting multiple sclerosis: correlation with lesion load. NeuroImage 2003;18:360-366.

124. Roosendaal SD, Bendfeldt K, Vrenken H, et al. Grey matter volume in a large cohort of MS patients: relation to MRI parameters and disability. Mult Scler 2011;17:1098-1106.

125. Ceccarelli A, Rocca MA, Pagani E, et al. A voxel-based morphometry study of grey matter loss in MS patients with different clinical phenotypes. NeuroImage 2008;42:315-322.

126. Ceccarelli A, Rocca MA, Valsasina P, et al. A multiparametric evaluation of regional brain damage in patients with primary progressive multiple sclerosis. Human brain mapping 2009;30:3009-3019.

127. Sepulcre J, Sastre-Garriga J, Cercignani M, Ingle GT, Miller DH, Thompson AJ. Regional gray matter atrophy in early primary progressive multiple sclerosis: a voxel-based morphometry study. Archives of neurology 2006;63:1175-1180.

128. Fisher E, Lee JC, Nakamura K, Rudick RA. Gray matter atrophy in multiple sclerosis: a longitudinal study. Annals of neurology 2008;64:255-265.

129. Kidd D, Barkhof F, McConnell R, Algra PR, Allen IV, Revesz T. Cortical lesions in multiple sclerosis. Brain : a journal of neurology 1999;122 (Pt 1):17-26.

130. Geurts JJ, Pouwels PJ, Uitdehaag BM, Polman CH, Barkhof F, Castelijns JA. Intracortical lesions in multiple sclerosis: improved detection with 3D double inversion-recovery MR imaging. Radiology 2005;236:254-260.

131. Calabrese M, Rocca MA, Atzori M, et al. Cortical lesions in primary progressive multiple sclerosis: a 2-year longitudinal MR study. Neurology 2009;72:1330-1336.

132. Kalkers NF, Bergers E, Castelijns JA, et al. Optimizing the association between disability and biological markers in MS. Neurology 2001;57:1253-1258.

133. Nijeholt GJ, van Walderveen MA, Castelijns JA, et al. Brain and spinal cord abnormalities in multiple sclerosis. Correlation between MRI parameters, clinical subtypes and symptoms. Brain : a journal of neurology 1998;121 (Pt 4):687-697.

134. Miller DH, Barkhof F, Frank JA, Parker GJ, Thompson AJ. Measurement of atrophy in multiple sclerosis: pathological basis, methodological aspects and clinical relevance. Brain : a journal of neurology 2002;125:1676-1695.

135. Rovaris M, Judica E, Sastre-Garriga J, et al. Large-scale, multicentre, quantitative MRI study of brain and cord damage in primary progressive multiple sclerosis. Mult Scler 2008;14:455-464.

136. Fisniku LK, Chard DT, Jackson JS, et al. Gray matter atrophy is related to long-term disability in multiple sclerosis. Annals of neurology 2008;64:247-254.

137. Sanfilipo MP, Benedict RH, Weinstock-Guttman B, Bakshi R. Gray and white matter brain atrophy and neuropsychological impairment in multiple sclerosis. Neurology 2006;66:685-692.

138. Riccitelli G, Rocca MA, Pagani E, et al. Cognitive impairment in multiple sclerosis is associated to different patterns of gray matter atrophy according to clinical phenotype. Human brain mapping 2011;32:1535-1543.

139. Kalkers NF, Ameziane N, Bot JC, Minneboo A, Polman CH, Barkhof F. Longitudinal brain volume measurement in multiple sclerosis: rate of brain atrophy is independent of the disease subtype. Archives of neurology 2002;59:1572-1576.

140. Peterson JW, Bo L, Mork S, Chang A, Trapp BD. Transected neurites, apoptotic neurons, and reduced inflammation in cortical multiple sclerosis lesions. Annals of neurology 2001;50:389-400.

141. Dalton CM, Chard DT, Davies GR, et al. Early development of multiple sclerosis is associated with progressive grey matter atrophy in patients presenting with clinically isolated syndromes. Brain : a journal of neurology 2004;127:1101-1107.

142. Tiberio M, Chard DT, Altmann DR, et al. Gray and white matter volume changes in early RRMS: a 2-year longitudinal study. Neurology 2005;64:1001-1007.

143. Saindane AM, Ge Y, Udupa JK, Babb JS, Mannon LJ, Grossman RI. The effect of gadolinium-enhancing lesions on whole brain atrophy in relapsing-remitting MS. Neurology 2000;55:61-65.

144. Fisher E, Rudick RA, Simon JH, et al. Eight-year follow-up study of brain atrophy in patients with MS. Neurology 2002;59:1412-1420.

145. Hardmeier M, Wagenpfeil S, Freitag P, et al. Atrophy is detectable within a 3-month period in untreated patients with active relapsing remitting multiple sclerosis. Archives of neurology 2003;60:1736-1739.

146. Paolillo A, Piattella MC, Pantano P, et al. The relationship between inflammation and atrophy in clinically isolated syndromes suggestive of multiple sclerosis: a monthly MRI study after triple-dose gadolinium-DTPA. Journal of neurology 2004;251:432-439.

147. Inglese M, Mancardi GL, Pagani E, et al. Brain tissue loss occurs after suppression of enhancement in patients with multiple sclerosis treated with autologous haematopoietic stem cell transplantation. Journal of neurology, neurosurgery, and psychiatry 2004;75:643-644.

148. Vercellino M, Masera S, Lorenzatti M, et al. Demyelination, inflammation, and neurodegeneration in multiple sclerosis deep gray matter. Journal of neuropathology and experimental neurology 2009;68:489-502.

149. Inglese M, Rovaris M, Giacomotti L, Mastronardo G, Comi G, Filippi M. Quantitative brain volumetric analysis from patients with multiple sclerosis: a follow-up study. Journal of the neurological sciences 1999;171:8-10.

150. Leigh R, Ostuni J, Pham D, et al. Estimating cerebral atrophy in multiple sclerosis patients from various MR pulse sequences. Mult Scler 2002;8:420-429.

151. Horsfield MA, Rovaris M, Rocca MA, et al. Whole-brain atrophy in multiple sclerosis measured by two segmentation processes from various MRI sequences. Journal of the neurological sciences 2003;216:169-177.

152. Leary SM, Davie CA, Parker GJ, et al. 1H magnetic resonance spectroscopy of normal appearing white matter in primary progressive multiple sclerosis. Journal of neurology 1999;246:1023-1026.

153. Suhy J, Rooney WD, Goodkin DE, et al. 1H MRSI comparison of white matter and lesions in primary progressive and relapsing-remitting MS. Mult Scler 2000;6:148-155.

154. Cucurella MG, Rovira A, Rio J, et al. Proton magnetic resonance spectroscopy in primary and secondary progressive multiple sclerosis. NMR in biomedicine 2000;13:57-63.

155. Fernando KT, McLean MA, Chard DT, et al. Elevated white matter myo-inositol in clinically isolated syndromes suggestive of multiple sclerosis. Brain : a journal of neurology 2004;127:1361-1369.

156. Allen IV, McKeown SR. A histological, histochemical and biochemical study of the macroscopically normal white matter in multiple sclerosis. Journal of the neurological sciences 1979;41:81-91.

157. Shen J, Petersen KF, Behar KL, et al. Determination of the rate of the glutamate/glutamine cycle in the human brain by in vivo 13C NMR. Proceedings of the National Academy of Sciences of the United States of America 1999;96:8235-8240.

158. Petroff OA, Pleban LA, Spencer DD. Symbiosis between in vivo and in vitro NMR spectroscopy: the creatine, N-acetylaspartate, glutamate, and GABA content of the epileptic human brain. Magnetic resonance imaging 1995;13:1197-1211.

159. Griffin JL, Bollard M, Nicholson JK, Bhakoo K. Spectral profiles of cultured neuronal and glial cells derived from HRMAS (1)H NMR spectroscopy. NMR in biomedicine 2002;15:375-384.

160. Pan JW, Coyle PK, Bashir K, Whitaker JN, Krupp LB, Hetherington HP. Metabolic differences between multiple sclerosis subtypes measured by quantitative MR spectroscopy. Mult Scler 2002;8:200-206.

161. Sarchielli P, Presciutti O, Pelliccioli GP, et al. Absolute quantification of brain metabolites by proton magnetic resonance spectroscopy in normal-appearing white matter of multiple sclerosis patients. Brain : a journal of neurology 1999;122 (Pt 3):513-521.

162. De Stefano N, Matthews PM, Fu L, et al. Axonal damage correlates with disability in patients with relapsing-remitting multiple sclerosis. Results of a longitudinal magnetic resonance spectroscopy study. Brain : a journal of neurology 1998;121 (Pt 8):1469-1477.

163. Tiberio M, Chard DT, Altmann DR, et al. Metabolite changes in early relapsing-remitting multiple sclerosis. A two year follow-up study. Journal of neurology 2006;253:224-230.

164. Sajja BR, Narayana PA, Wolinsky JS, Ahn CW. Longitudinal magnetic resonance spectroscopic imaging of primary progressive multiple sclerosis patients treated with glatiramer acetate: multicenter study. Mult Scler 2008;14:73-80.

165. Chard DT, McLean MA, Parker GJ, MacManus DG, Miller DH. Reproducibility of in vivo metabolite quantification with proton magnetic resonance spectroscopic imaging. Journal of magnetic resonance imaging : JMRI 2002;15:219-225.

166. Geurts JJ, Barkhof F, Castelijns JA, Uitdehaag BM, Polman CH, Pouwels PJ. Quantitative 1H-MRS of healthy human cortex, hippocampus, and thalamus:

metabolite concentrations, quantification precision, and reproducibility. Journal of magnetic resonance imaging : JMRI 2004;20:366-371.

167. Maudsley AA, Domenig C, Sheriff S. Reproducibility of serial whole-brain MR spectroscopic imaging. NMR in biomedicine 2010;23:251-256.

168. Narayanan S, De Stefano N, Francis GS, et al. Axonal metabolic recovery in multiple sclerosis patients treated with interferon beta-1b. Journal of neurology 2001;248:979-986.

12. ADDENDUM (publications from this thesis)

1) Sastre-Garriga J, Ingle GT, Chard DT, Ramió-Torrentà L, Miller DH, Thompson AJ. Grey and white matter atrophy in early clinical stages of primary progressive multiple sclerosis. Neuroimage. 2004 May; 22(1):353-9. PubMed PMID: 15110026.

2) Sastre-Garriga J, Ingle GT, Chard DT, Cercignani M, Ramió-Torrentà L, Miller DH, Thompson AJ. Grey and white matter volume changes in early primary progressive multiple sclerosis: a longitudinal study. Brain. 2005 Jun; 128(Pt 6):1454-60.

3) Sastre-Garriga J, Ingle GT, Chard DT, Ramió-Torrentà L, McLean MA, Miller DH, Thompson AJ. Metabolite changes in normal-appearing gray and white matter are linked with disability in early primary progressive multiple sclerosis. Arch Neurol. 2005 Apr;62(4):569-73.